Magnetic reconnection in the fluid limit: connecting micro-scales to macroscopic dynamics.

Vyacheslav (Slava) Lukin

Space Science Division, US Naval Research Laboratory

Workshop on Computational Challenges in Magnetized Plasma
Institute for Pure and Applied Mathematics, UCLA
April 16th - 20th, 2012

Outline

- A few basic plasma reminders...
- Examples of Magnetic Reconnection in Lab, Space, and Theory
- Simple 2D Reconnection: A sampler of a few fluid systems
- Simple 3D Reconnection: Just a bit more complicated...

Plasma: Kinetic, Fluid, Magnetized Fluid

Kinetic Plasma

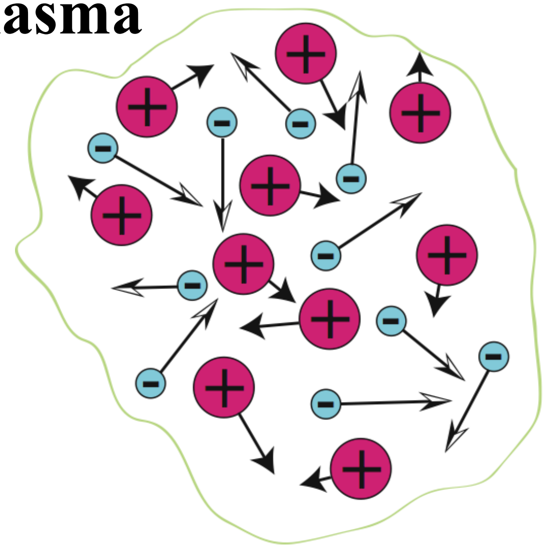

Fluid Plasma

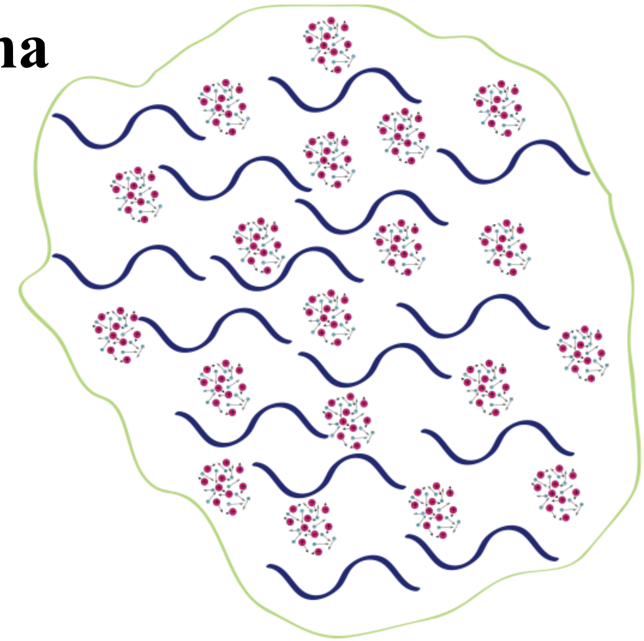

Magnetized Fluid Plasma

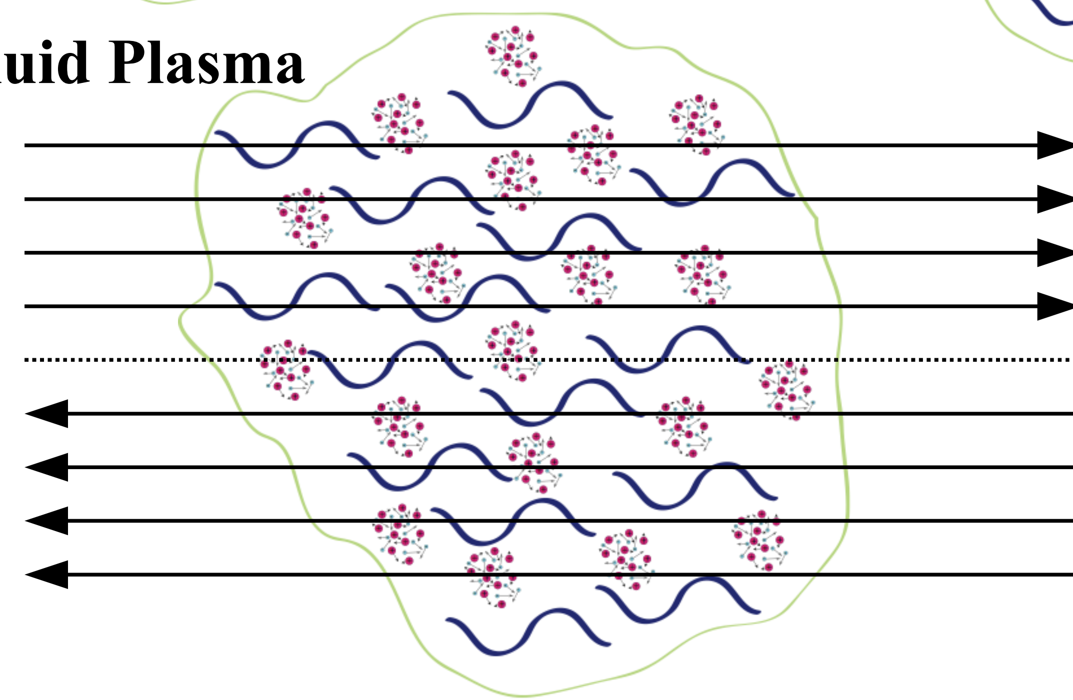

Kinetic-Fluid Connection

Boltzmann Equation for $f(t,\mathbf{x},\mathbf{v})$ in the <u>*6-dimensional*</u> $\{\mathbf{x},\mathbf{v}\}$ parameter space

$$\frac{\partial f}{\partial t} + \frac{\partial f}{\partial \mathbf{x}} \cdot \mathbf{v} + \frac{q}{m}\frac{\partial f}{\partial \mathbf{v}} \cdot \mathbf{F}(\mathbf{v}, \mathbf{E}, \mathbf{B}) = \left.\frac{\partial f}{\partial t}\right|_{coll}$$

together with the set of electro-magnetic Maxwell Equations provide the connection between the *kinetic* and *fluid* descriptions of a plasma.

Taking *velocity moments* of the Boltzmann Equation (essentially multiplying by powers of **v** and integrating over **v**) leads to the fluid equations that can be solved in the <u>*3-dimensional*</u> space as functions of time.

Only by making some assumptions about $f(\mathbf{v})$ can we end up with a reasonable number (a few) of *coupled nonlinear partial differential equations* (PDEs) that will fully describe the behavior of a plasma fluid.

Fluid Description of Plasma

In general, plasma can be treated as a fluid when the following conditions are satisfied:

When macroscopic dynamical time-scales are much longer than the longest collisional time-scale, i.e.:

$$(\delta/\delta t) \ll (1/\tau_{coll}),$$

AND macroscopic spatial scales are much larger than the mean free path, i.e.:

$$L \gg v_{th}\tau_{coll}$$

Some Classic and Recent References:

- *S. I. Braginskii*, "Transport processes in a plasma", Reviews of Plasma Physics, Vol. 1 (Consultants Bureau, New York, 1965);
- *D. Biskamp*, "Nonlinear Magnetohydrodynamics" (Cambridge University Press, 1997);
- *J. P. Goedbloed, R. Keppens, S. Poedts*, "Advanced Magnetohydrodynamics: With Applications to Laboratory and Astrophysical Plasmas" (Cambridge University Press, 2010);
- *S. C. Jardin*, "Computational Methods in Plasma Physics" (Taylor & Francis Group, 2010).

Fluid Description of Plasma: Magnetization

Magnetic fields introduce spatial anisotropy and macroscopic connectivity into the plasma. In particular, in a magnetized plasma validity of the classical fluid description is limited to systems where:

parallel gradient scales are much longer than the mean free path, i.e.:

$$L_{||} \gg v_{th}\tau_{coll}$$

AND perpendicular gradient scales are much longer than the particle Larmor radius, i.e.:

$$L_{\perp} \gg r_L$$

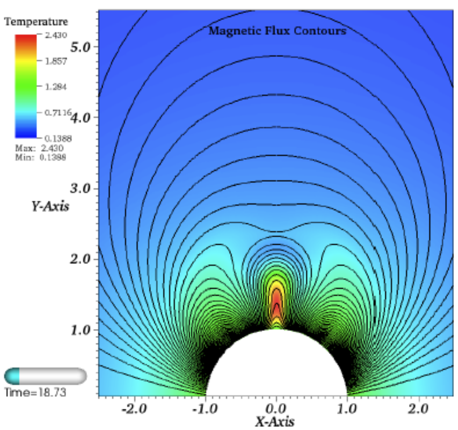

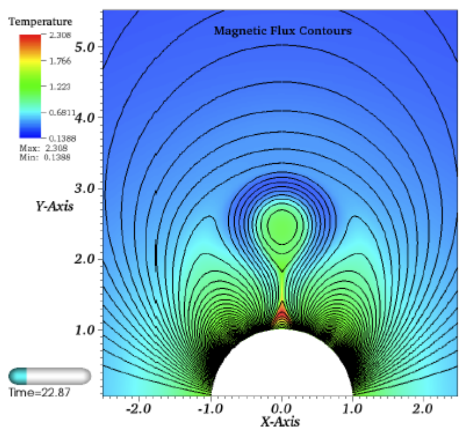

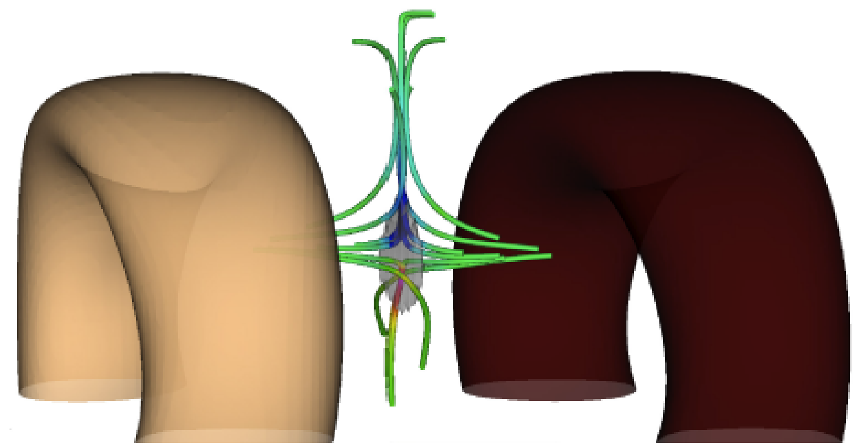

Fluid Description of Plasma: MHD

One of the simpler and most common fluid approximations for magnetized collisional plasma is the set of single-fluid compressible MagnetoHydroDynamic (MHD) PDEs that can be expressed as follows:

$$
\begin{aligned}
\frac{\partial \rho}{\partial t} &+ \nabla \cdot [\rho \mathbf{v}] = 0 \\
\frac{\partial (\rho \mathbf{v})}{\partial t} &+ \nabla \cdot \left[\rho \mathbf{v}\mathbf{v} + p\bar{\mathbf{I}} - \Pi\right] = \boxed{\mathbf{J} \times \mathbf{B}} \\
\mathbf{E} &= \boxed{-\mathbf{v} \times \mathbf{B}} + \mathbf{D}_J \\
\frac{1}{\gamma - 1}\frac{\partial p}{\partial t} &+ \nabla \cdot \left[\frac{\gamma}{\gamma - 1} p\mathbf{v} - \mathbf{Q}\right] = \mathbf{v} \cdot \nabla p + \Pi : \nabla \mathbf{v} + \mathbf{D}_J \cdot \mathbf{J}
\end{aligned}
$$

where γ is the adiabatic constant, Π is the viscous tensor, $\mathbf{D}_J$ is the magnetic diffusion operator, $\mathbf{Q}$ is the heat flux, and $\mathbf{E}$, $\mathbf{B}$ and $\mathbf{J}$ are related through Maxwell's equations.

Magnetic Reconnection

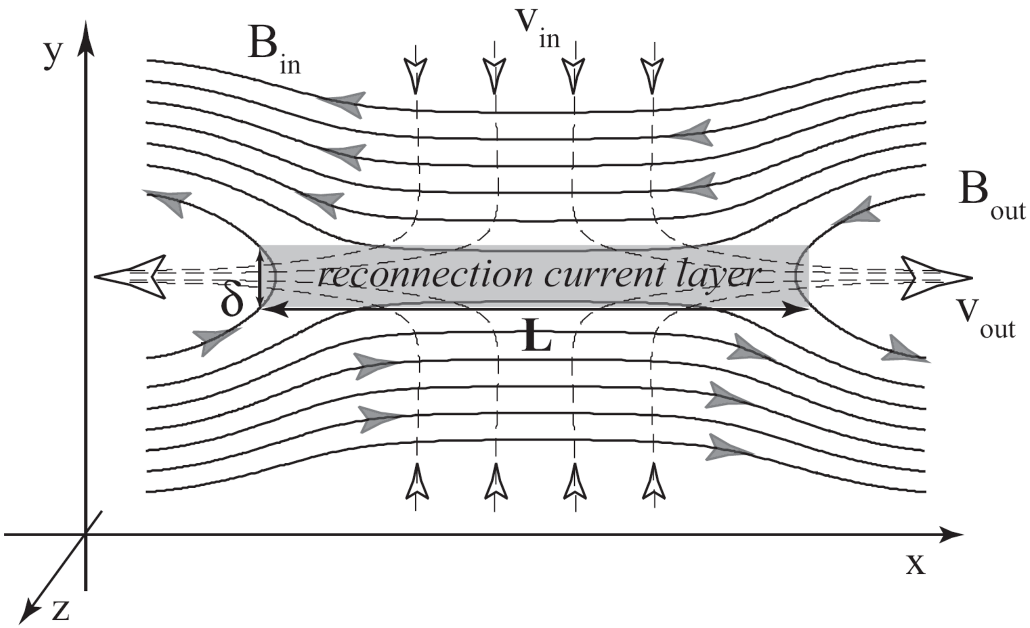

➢ Local reconfiguration and annihilation of magnetic fields resulting in relaxation of the global topology of a magnetic configuration in such a way as to transfer energy stored in the stressed magnetic fields into kinetic (directed) and thermal (random) energy of the plasma.

Where does/could magnetic reconnection play a role?

Astrophysics:

- pulsar magnetospheres
- heating of interstellar and intergalactic medium
- dynamics of accreting systems

Solar physics:

- solar flares, coronal mass ejections
- solar corona heating
- interaction of solar wind with the Earth magnetosphere

Magnetic Fusion Devices:

- sawtooth crash and tearing instability in toroidal devices
- coaxial helicity injection
- self-reversal in Reversed-Field Pinch devices

Magnetic Reconnection – Experiment

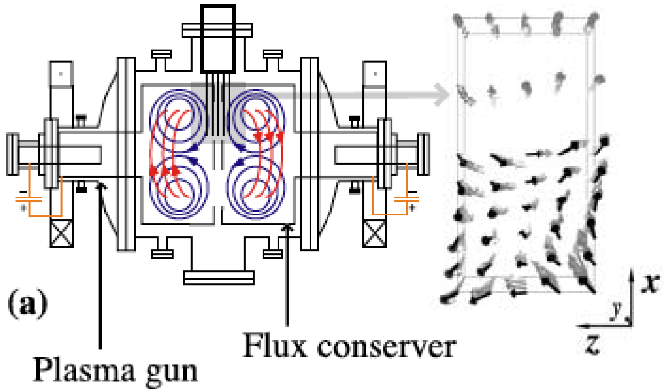

Swarthmore Spheromak eXperiment
Cothran, *et al.*, GRL (2003)

LArge Plasma Device
Lawrence & Gekelman
PRL (2009)

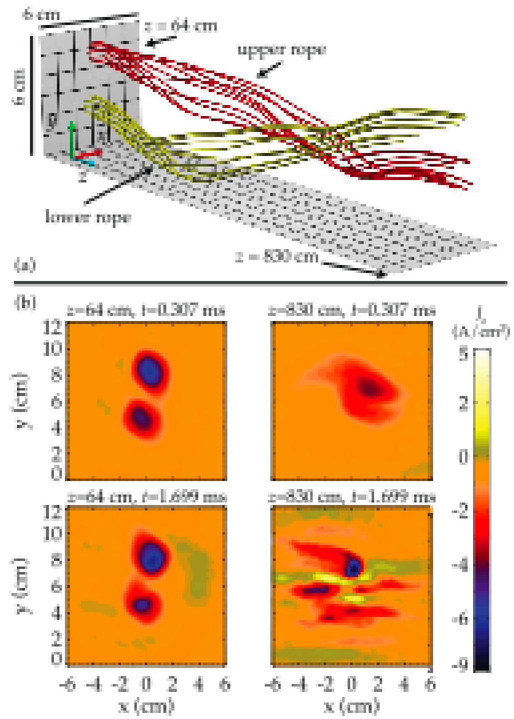

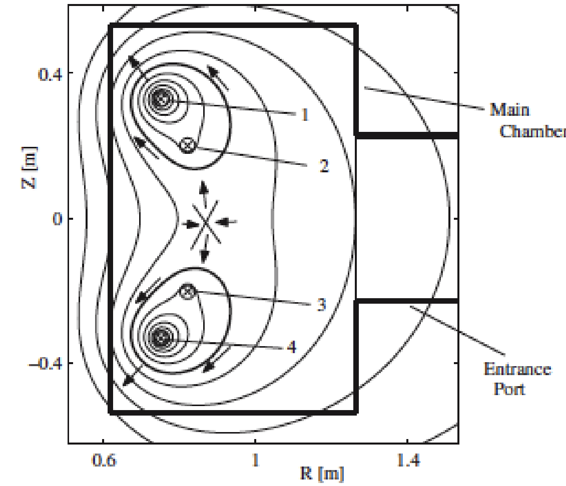

Versatile Toroidal Facility
Egedal, *et al.*, PRL (2007)

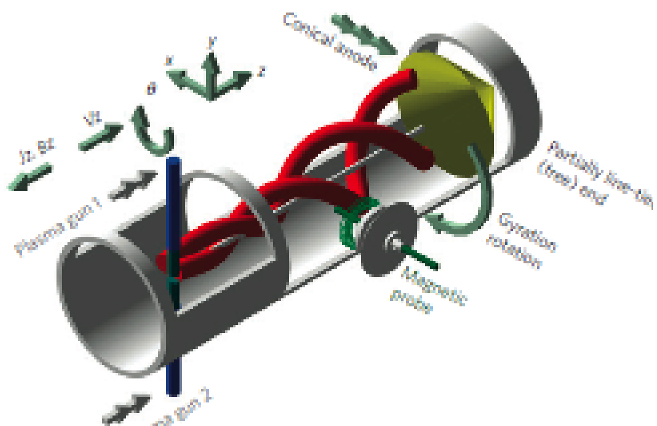

Reconnection Scaling eXperiment
Intrator, *et al.*,
Nature Physics (2009)

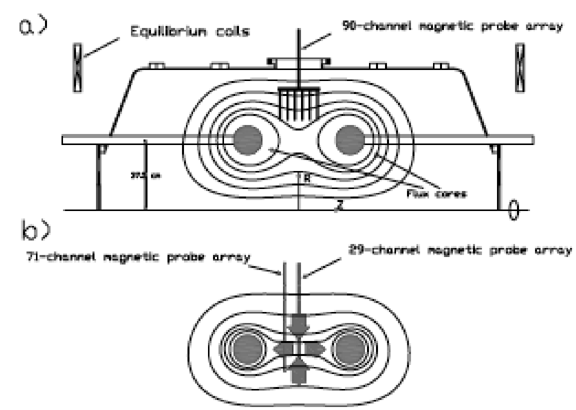

Magnetic Reconnection
eXperiment
Ren, *et al.*, PRL (2005)

Magnetic Reconnection – Magnetosphere

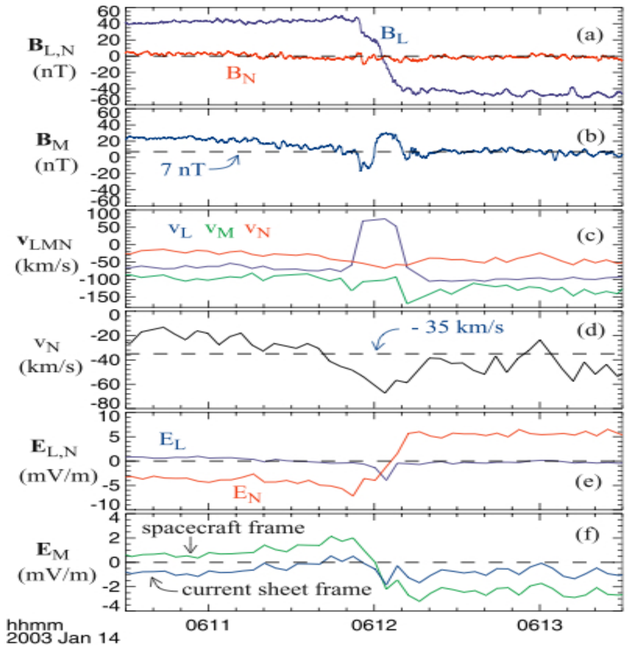

Figure 2. Cluster-1 data around the exhaust in the LMN coordinate system. (a) Anti-parallel, L, and normal, N, components of the magnetic field, (b) 'out-of-plane', M, magnetic field, (c) LMN components of the proton velocity, (d) expanded plot of the proton flow component normal to the current sheet, (e) L and N components of the electric field, and (f) M component of the electric field in the spacecraft frame (green) and in the current sheet frame moving at −35 km/s along the normal (blue).

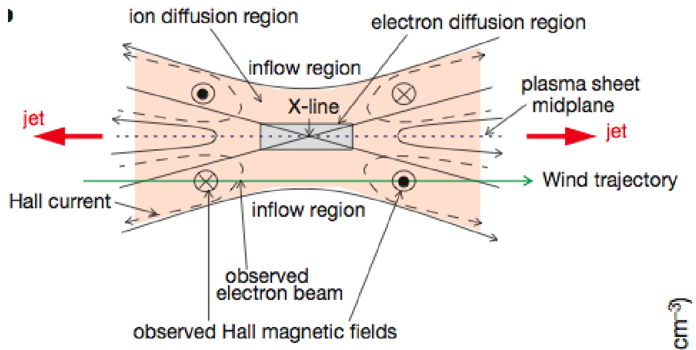

Magnetotail Reconnection
(Wind spacecraft)
Øieroset, *et al.*, Nature (2001)

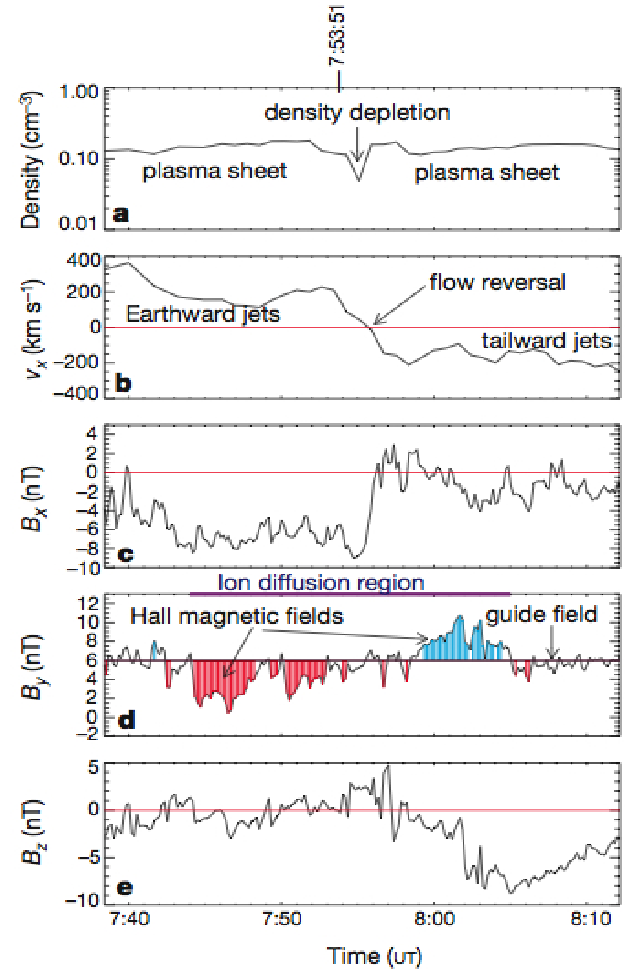

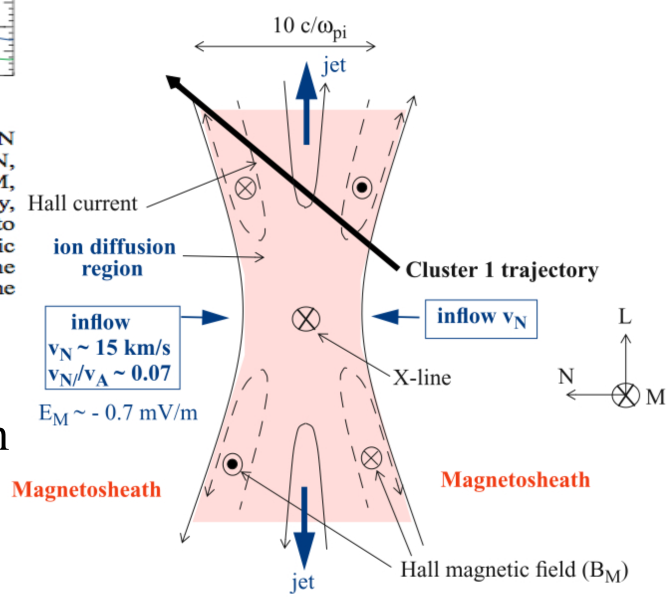

Magnetosheath Reconnection
(Cluster 1 spacecraft)
Phan *et al.*, GRL (2007)

Magnetic Reconnection – Solar

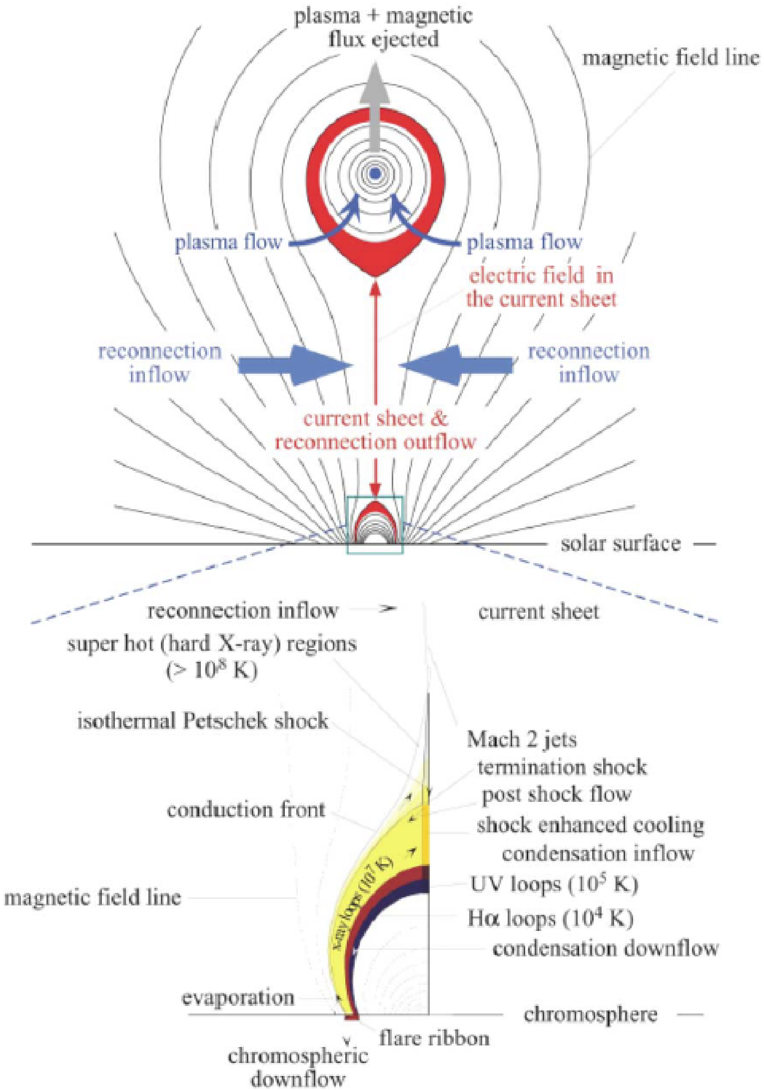

Post-CME Current Sheets
Lin, *et al.*, JGR (2008)

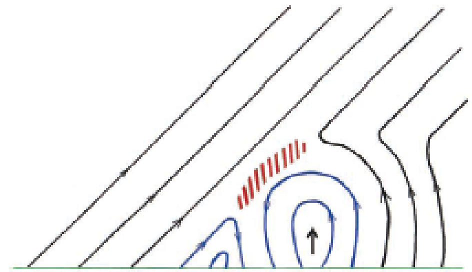

Impulsive Flares
Reames, ApJL (2002)

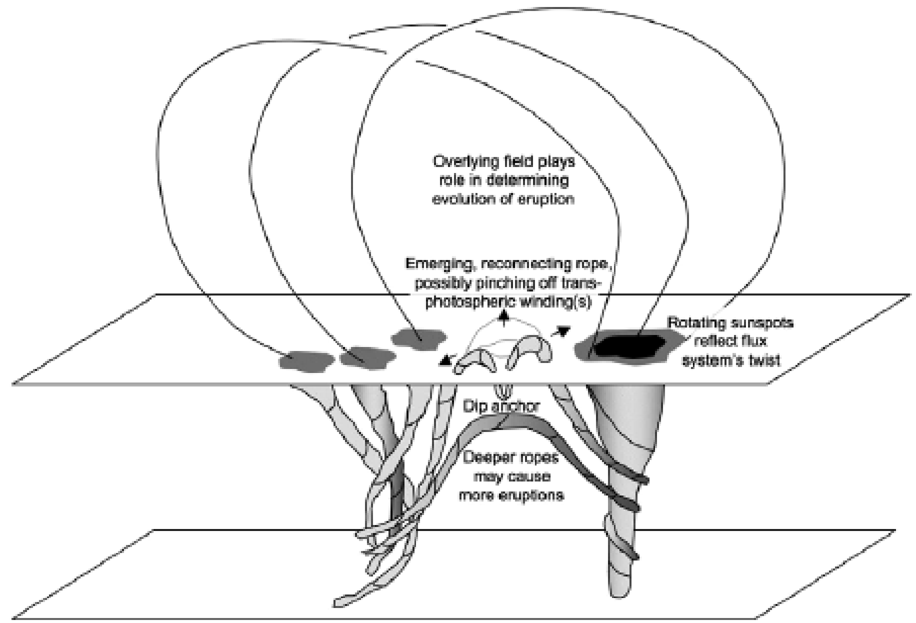

Flux Emergence and
Chromospheric Reconnection
Schrijver, Adv. Space Res. (2009)

Magnetic Reconnection – 2D Fluid Theory

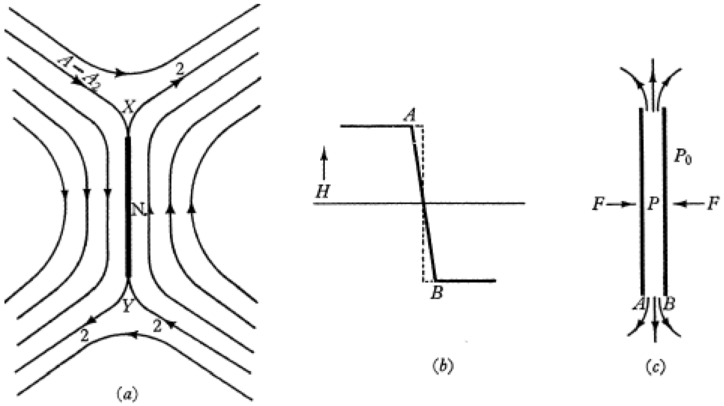

Fig. 5. The collision layer. (a) Field in neighbourhood of current sheet. (b) Field across current sheet. (c) Idealized hydrodynamic model.

Resistive MHD Analysis
Sweet, Nuovo Cimento (1958)

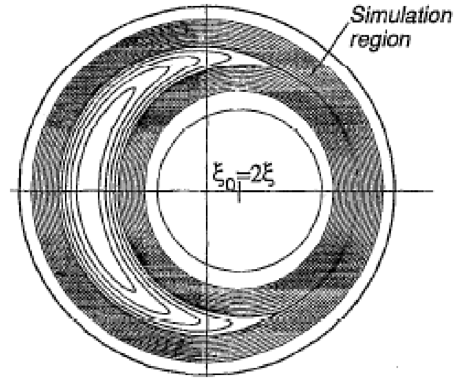

Two-Fluid (ion+electron) Simulations
Rogers & Zakharov, PoP (1995)

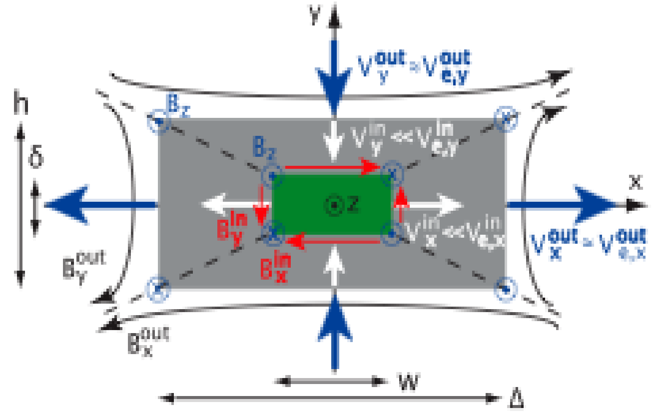

Hall MHD Analysis
Simakov & Chacon, PRL (2008)

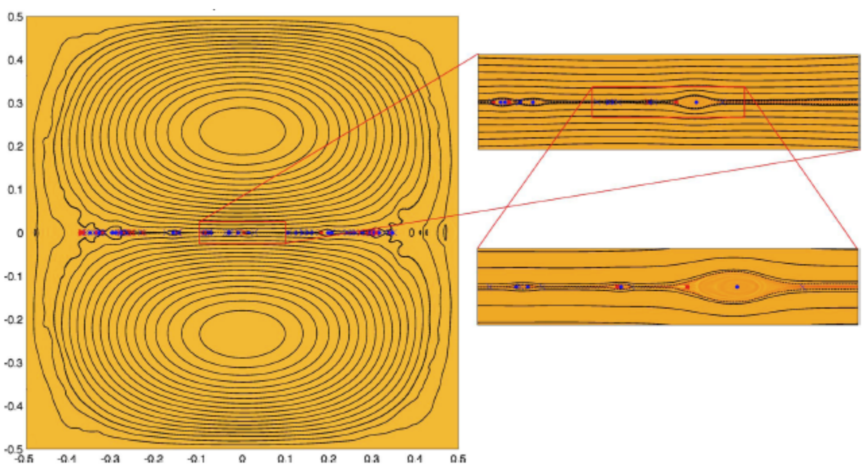

Plasmoid-Facilitated Reconnection
Huang & Bhattacharjee, PoP (2010)

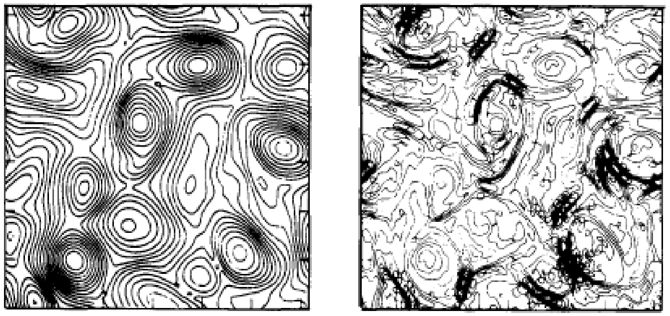

Reconnection in MHD Turbulence
Matthaeus & Lamkin, PoF (1986)

Magnetic Reconnection – 3D Fluid Theory

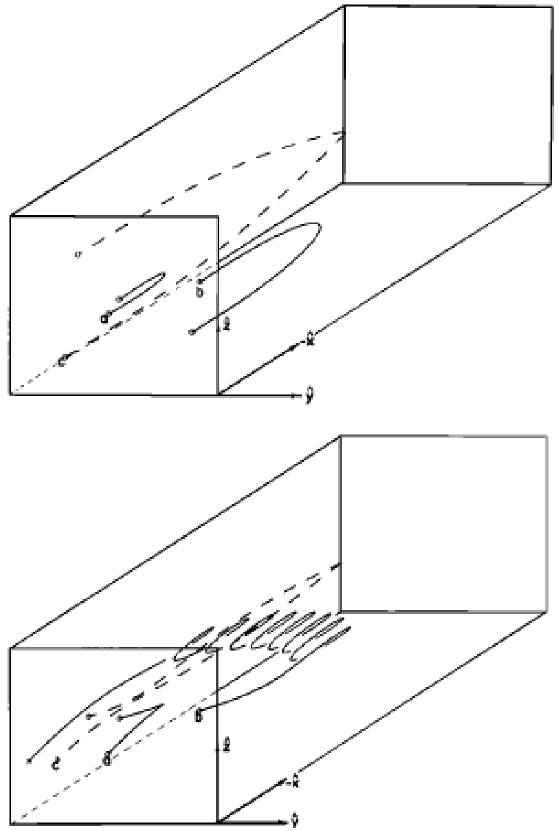

Helicity and Generalized
3D Reconnection
Schindler, *et al.*, JGR (1988)

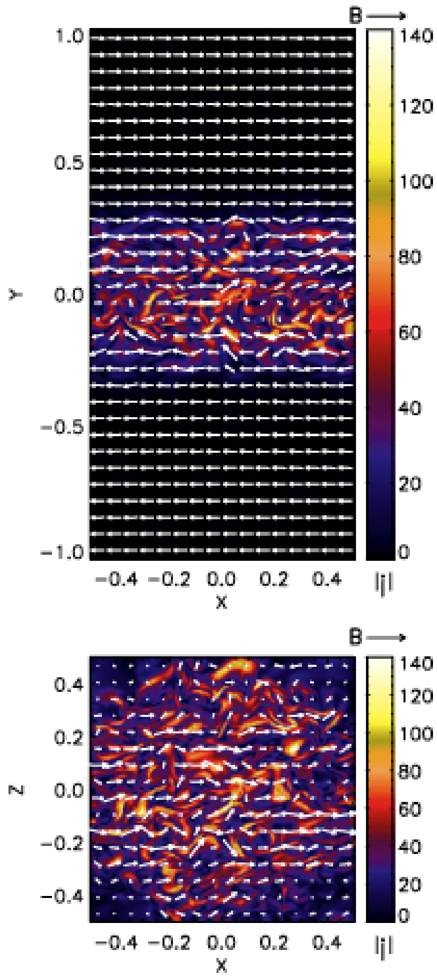

Turbulence in
Reconnection
Kowal *et al.*,
ApJ (2009)

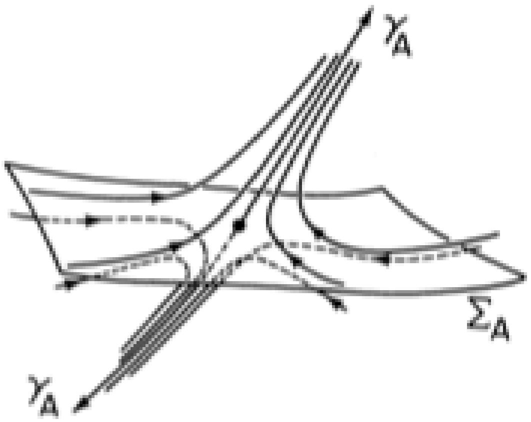

Topology Classification
Lau & Finn, ApJ (1990)

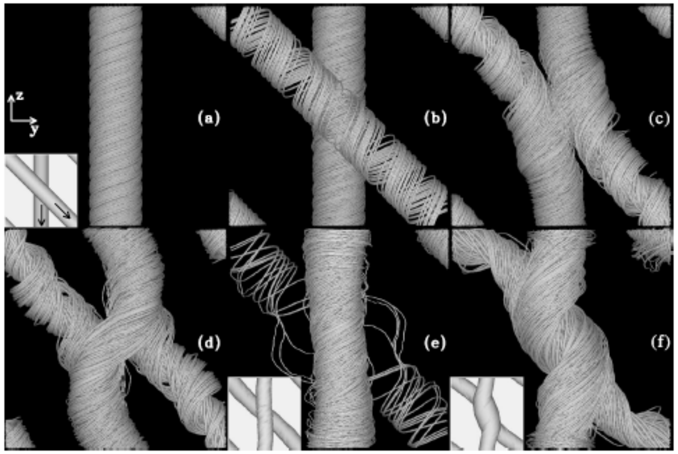

Flux-Tube Interaction Simulations
Linton & Antiochos, ApJ (2005)

Self-Organization & Relaxation

Selective Decay Hypothesis
Matthaeus & Montgomery
Ann. N.Y. Acad. Sci. (1980)

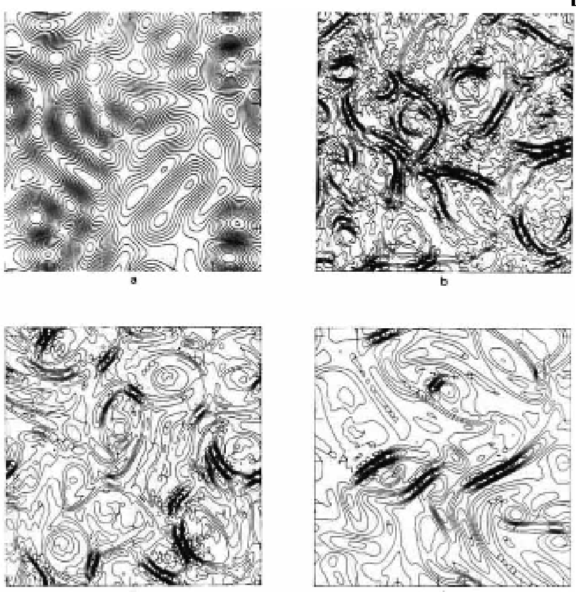

Woltjer-Taylor Conjecture:

Magnetized plasmas in closed systems relax towards
$\nabla \times \mathbf{B} = \lambda \mathbf{B}$,
with lowest uniform λ
satisfying boundary conditions.
Woltjer, Proc. Nat. Acad. Sci. (1958) & Taylor, PRL (1974).

Key Quantities to Consider:

Magnetic Energy
$$W_M \equiv \frac{1}{2} \int_V \mathbf{B} \cdot \mathbf{B} dV$$

Magnetic Helicity
$$K \equiv \int_V \mathbf{A} \cdot \mathbf{B} dV$$

$$< \lambda > \equiv (2W_M / K)$$

Cross-Helicity
$$H_C \equiv \int_V \mathbf{v} \cdot \mathbf{B} dV$$

...

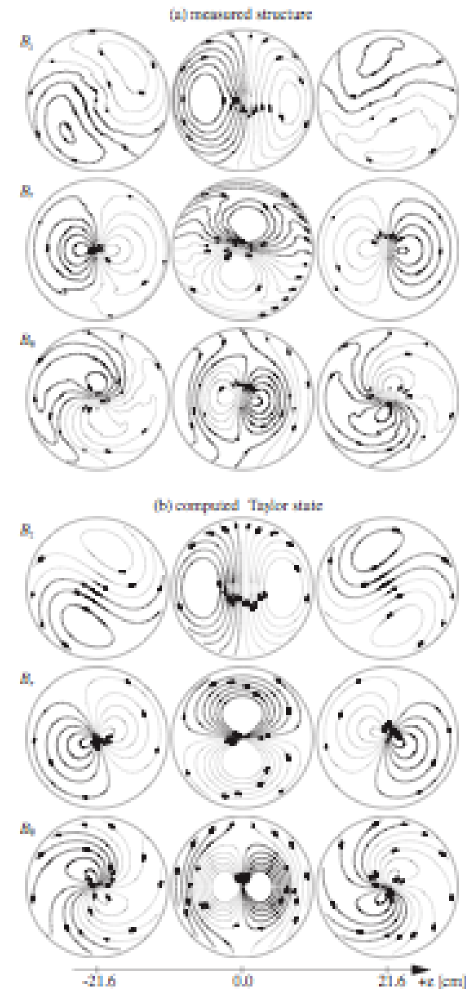

Cothran, *et al.*, PRL (2009)

So, When Is There (No) Reconnection?

- In vacuum (or neutral gas medium), there is nothing to stress magnetic field-lines and thus magnetic fields can simply annihilate without energy release;
- In ideal MHD – in particular, in the absence of magnetic diffusion – the magnetic field lines are "frozen-in" into perfectly conducting fluid elements and cannot reconnect: magnetic topology is exactly preserved and infinitely thin and strong current layers may result between stressed magnetic lines that cannot relax within the given topology;
- In highly resistive systems, where magnetic diffusion of dynamically important perturbations is faster than convection on the global scale, the situation resembles that in vacuum. No small-scale structure forms, and magnetic field stresses are released diffusively on the global scale;
- **Definition of magnetic reconnection due to Axford (1984) adopted by Schindler *et al.* (1988):** localized breakdown of the "frozen-in field" condition and the resulting changes of "connection" is the basis of magnetic reconnection. Here "connection" means that plasma elements which are at one time connected by a single magnetic field line remain connected at subsequent times.

Single-Fluid Resistive Reconnection

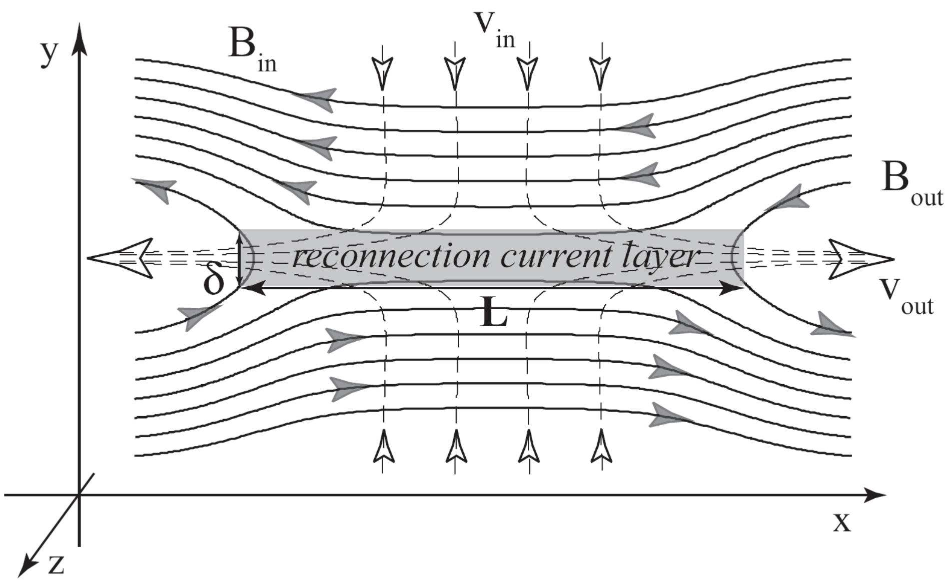

Uniform density, incompressible MHD:

$$\boxed{\begin{aligned} \frac{d\mathbf{v}}{dt} &= -\nabla p + \mathbf{J} \times \mathbf{B} \\ \mathbf{E} &= -\mathbf{v} \times \mathbf{B} + D(\eta, \mathbf{J}) \\ \frac{\partial B}{\partial t} &= -\nabla \times \mathbf{E} \\ \mathbf{J} &= \nabla \times \mathbf{B}. \end{aligned}}$$

Assume:

$$\omega \equiv (\delta/L) \ll 1 \quad \Rightarrow \quad \left\{ \begin{aligned} E_R = V_{in} B_{in} &= V_{out} B_{out} = D(\eta, J_0) \\ V_{in} L &= V_{out} \delta \\ V_{out} &= B_{in} \end{aligned} \right.$$

From these, another relationship follows:

Parker (1957), *Sweet* (1958)

$$E_R = \omega B_{in}^2 = D(\eta, J_0).$$

Uniform Resistivity Simulation

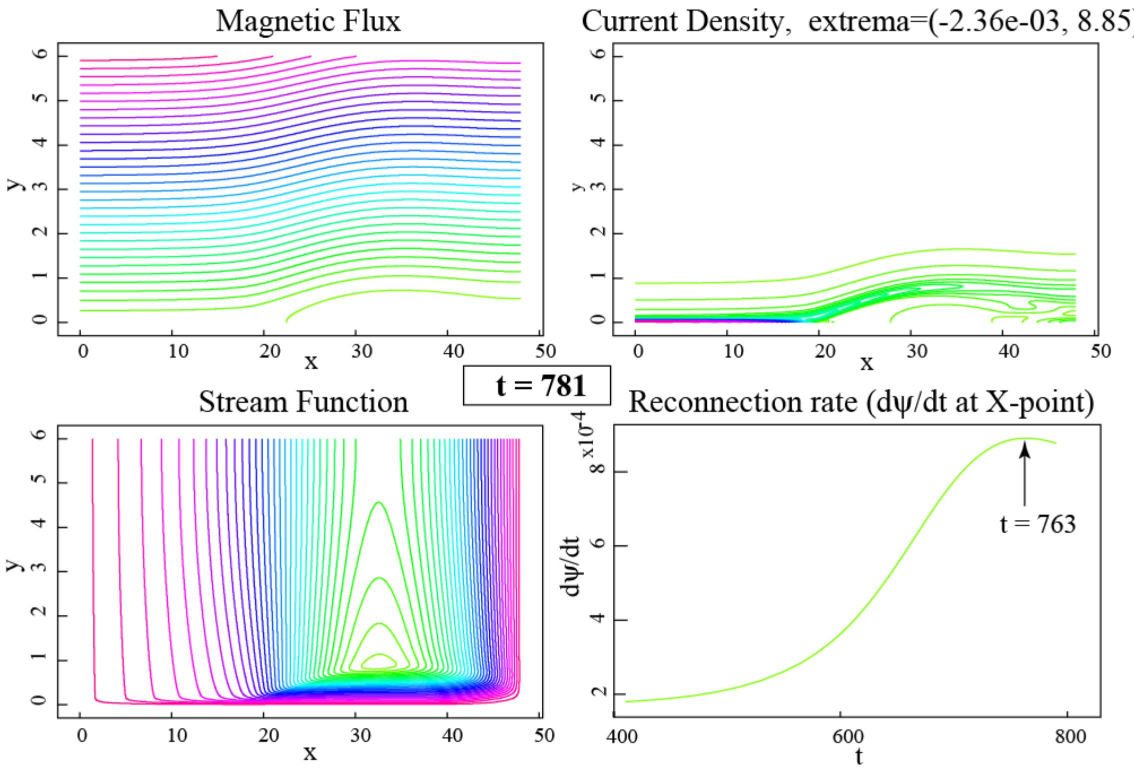

✓ Quarter-domain simulation utilizes symmetry of the problem;
✓ Localized perturbation in the lower-left corner of the domain initializes reconnection of the Harris-sheet equilibrium;
✓ "Open" boundary condition allows plasma inflow and bending of magnetic field-lines by fixing $B_x=1$ and $v_x=0$ on top boundary;
✓ System is periodic in the outflow x-direction.

Uniform resistivity: $D(\eta, \mathbf{J}) = \eta \mathbf{J}$

$$E_R = \frac{\eta^{1/2} B_{in}^{3/2}}{L^{1/2}}$$

Classical Sweet-Parker result of "slow" resistive reconnection with the reconnection current sheet elongating to the system size.

Anomalous Resistivity Model-I

Try anomalous resistive diffusion operator of the form

$$D(\eta, \mathbf{J}) = \begin{cases} \eta \mathbf{J}, & |\mathbf{J}| < J_c \\ \eta \left[1 + (|\mathbf{J}|/J_c - 1)^\alpha\right] \mathbf{J}, & |\mathbf{J}| \geq J_c \end{cases}$$

where J_c is some critical current density such that anomalous diffusion sets in when $|\mathbf{J}| \geq J_c$. In the limit of $|\mathbf{J}| \gg J_c$ and $\alpha \geq 1$, such diffusion operator can be approximated as

$$D(\eta, \mathbf{J}) \approx \eta (|\mathbf{J}|/J_c)^\alpha \mathbf{J}$$

with resulting reconnection rate of the form

$$E_R = \left[\frac{\eta B_{in}^{3(\alpha+1)}}{J_c^\alpha L^{\alpha+1}} \right]^{\frac{1}{\alpha+2}} .$$

Model-I Resistivity Simulation

Magnetic Flux

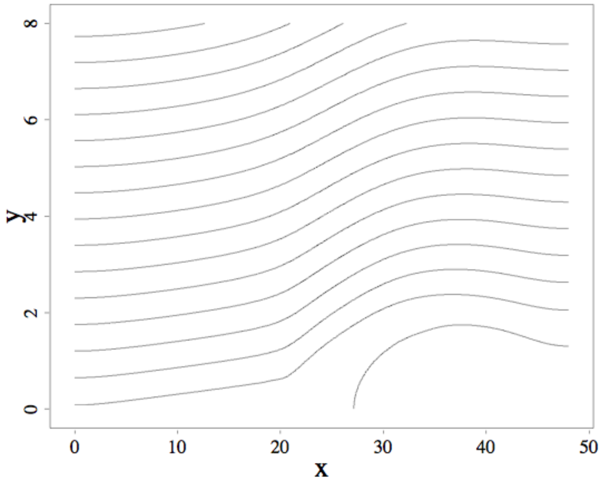

Reconnection Rate

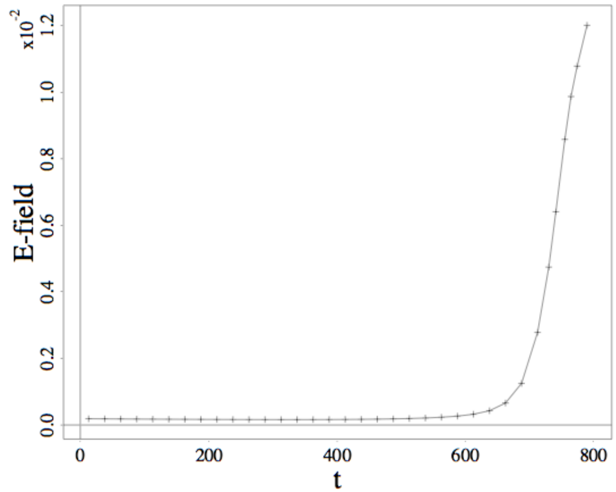

Current Density Profiles Across & Along the Reconnection Region

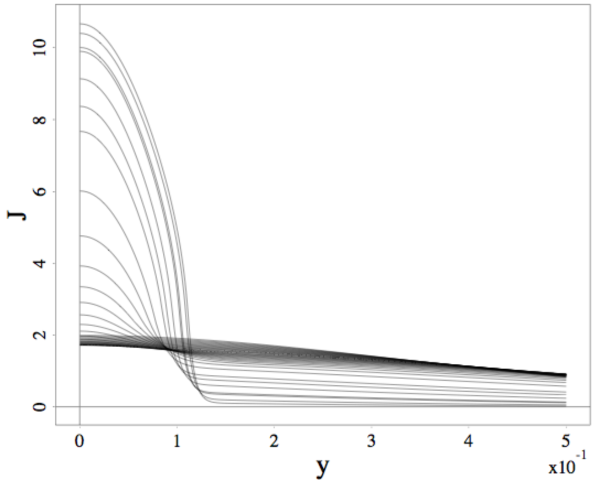

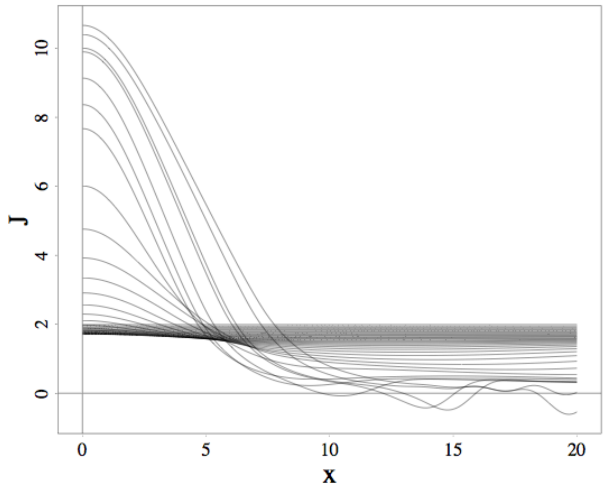

<u>Model-I anomalous resistivity simulation with</u>:

$$
\begin{aligned}
\alpha &= 2 \\
\eta &= 10^{-4} \\
J_c &= 2.5
\end{aligned}
$$

✓ Moderate opening up of the outflow channel and reconnection rate acceleration is apparent;

✓ Nevertheless, the current sheet continues to elongate and no signature of the reconnection region collapse is noticeable.

Anomalous Resistivity Model-II

Now, try a different anomalous resistive diffusion operator

$$D(\eta, \mathbf{J}) = \frac{\eta}{2}\left[1 + \frac{1}{\sqrt{1 - |\mathbf{J}/J_c|^2}}\right]\mathbf{J},$$

where $J_c > |\mathbf{J}|$ is some maximum allowable critical value of plasma current density such that anomalous resistivity becomes infinite as $|\mathbf{J}|$ approaches J_c. Physically, such qualitative behavior can be expected in systems where the reconnection current sheet becomes unstable to global 3D instabilities, e.g. kinking, whenever the plasma current density approaches J_c.

In the limit of $(|\mathbf{J}|/J_c) \to 1$, such diffusion operator can be approximated as

$$D \approx \frac{\eta}{2\sqrt{1 - |\mathbf{J}/J_c|^2}}\mathbf{J} = \frac{\eta}{2\epsilon}\mathbf{J},$$

where $\epsilon \equiv \sqrt{1 - |\mathbf{J}/J_c|^2} \ll 1$ and the resulting reconnection rate has the form

$$E_R = \left(\frac{\eta}{2\epsilon L}\right)^{1/2} B_{in}^{3/2}.$$

Model-II Resistivity Simulation

Magnetic Flux

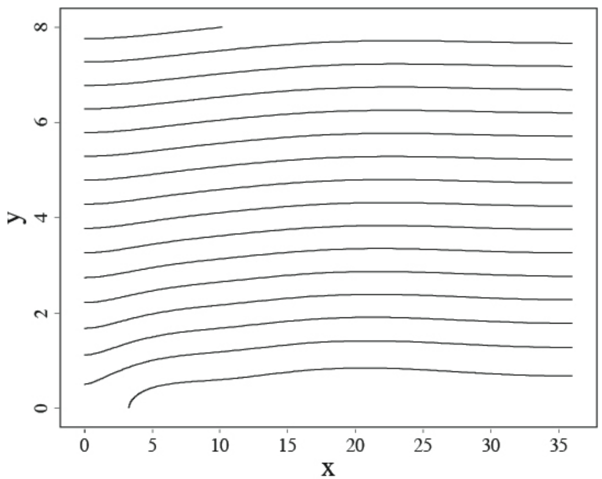

Reconnection Rate

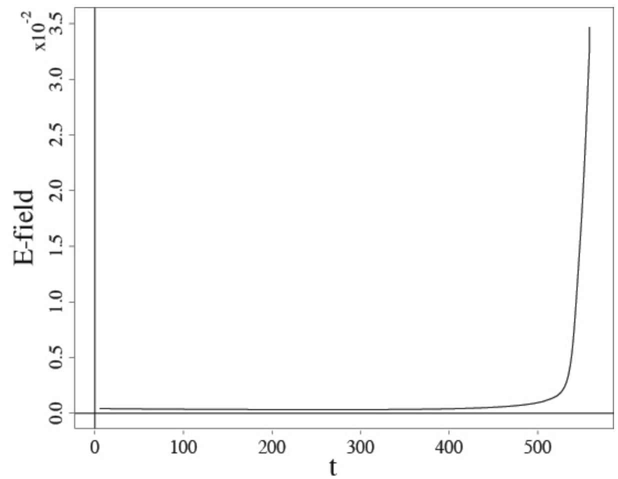

Current Density Profiles Across & Along the Reconnection Region

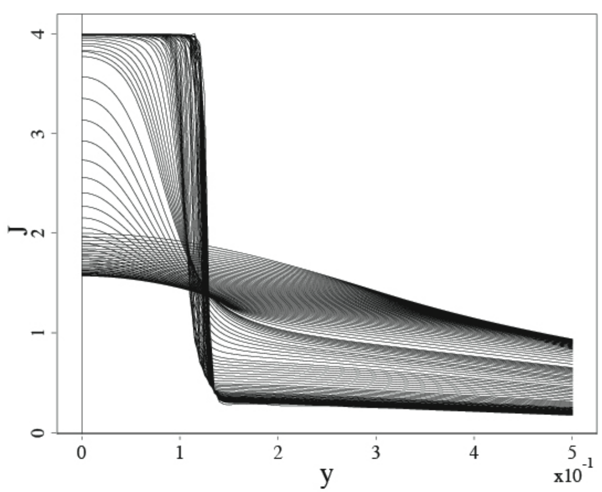

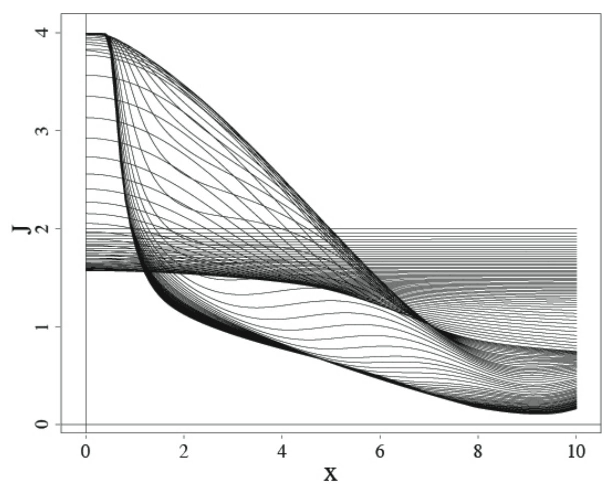

<u>Model-II anomalous resistivity simulation with</u>:

$$\eta = 2 * 10^{-4}$$
$$J_c = 4.0$$

✓ Greater opening up of the magnetic nozzle and explosive increase in the reconnection rate is evident;

✓ The current sheet collapses to an aspect ratio of L/δ ~ 10 as |**J**| begins to approach $J_{C.}$

Model-II Resistivity Simulation

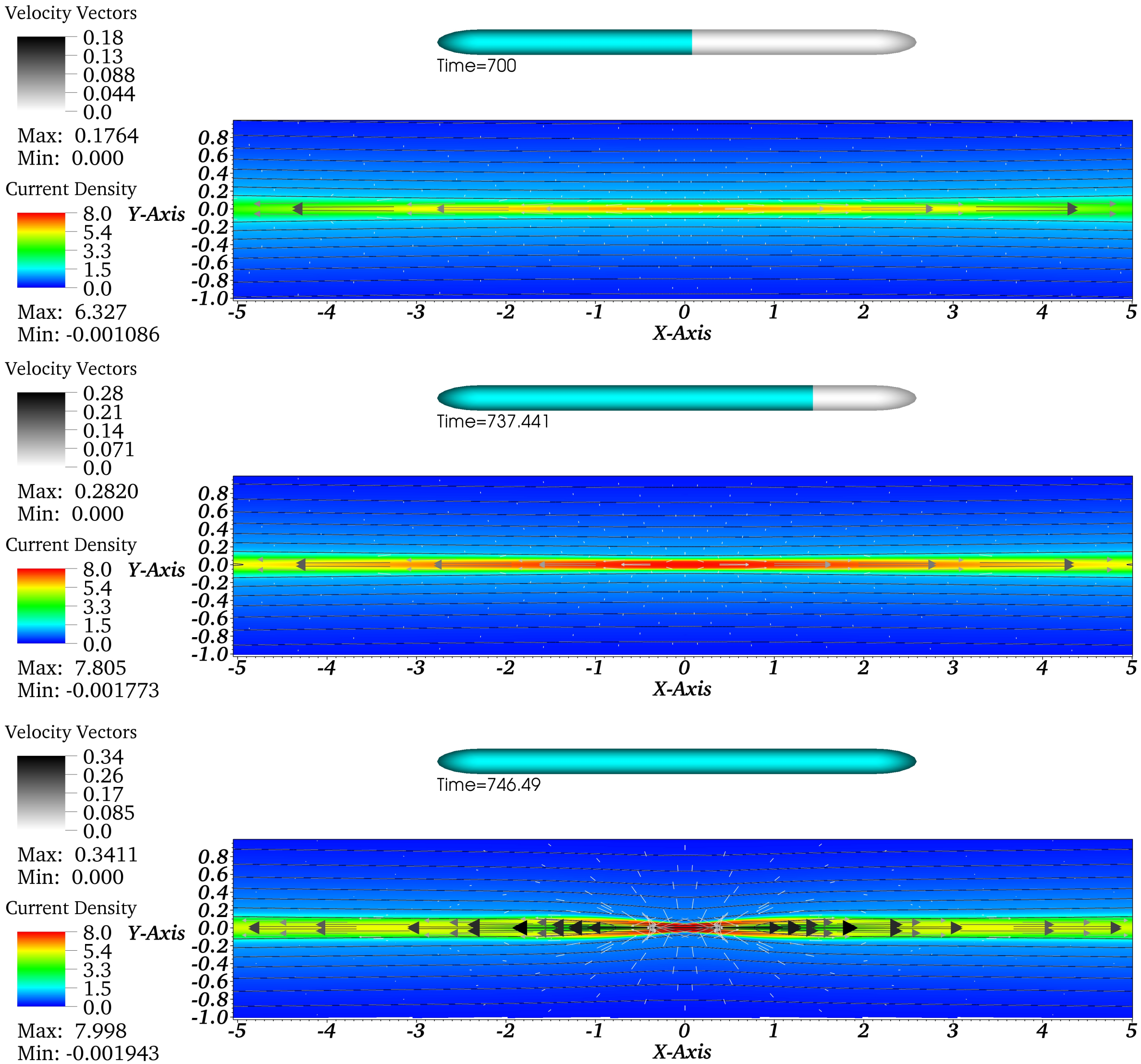

<u>Model-II anomalous resistivity simulation with</u>:

$$\eta = 10^{-4}$$
$$J_c = 8.0$$

- ✓ Opening up of the magnetic nozzle also correlated with explosive increase in the outflow velocity;
- ✓ As the main current sheet collapses, sharp and strong current layers form along the magnetic separatrices;

Two-Fluid (electron + positron) Reconnection

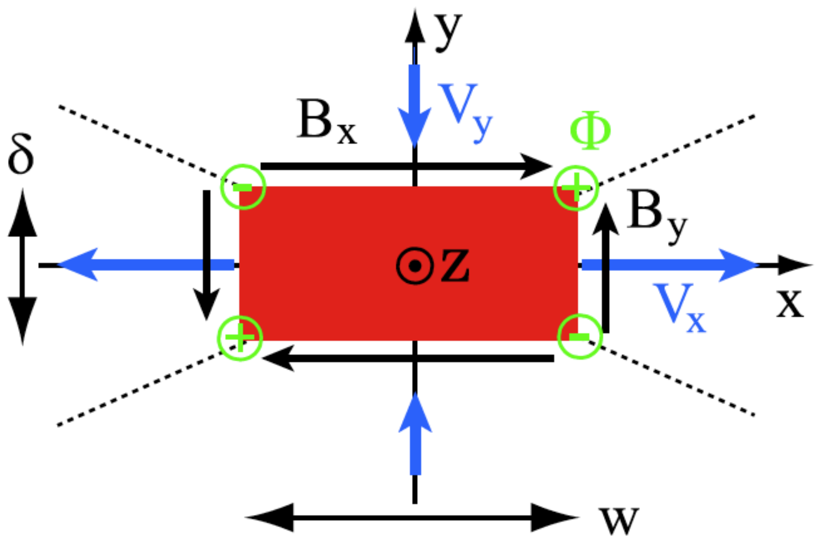

$$\partial_t \mathbf{v} + \mathbf{v}\cdot\nabla\mathbf{v} + \frac{d_e^2}{4}\mathbf{j}\cdot\nabla\mathbf{j} - \mu\nabla^2\mathbf{v} = \frac{\mathbf{j}\times\mathbf{B} - \nabla p}{2n},$$

$$\frac{d_e^2}{2}[\partial_t \mathbf{j} + \nabla\cdot(\mathbf{v}\mathbf{j} + \mathbf{j}\mathbf{v}) - \mu\nabla^2\mathbf{j}] = \mathbf{E} + \mathbf{v}\times\mathbf{B} - \eta\mathbf{j},$$

Chacon, et al., PRL (2008)

$$E_z \approx \frac{B_{x,\max}^2}{\sqrt{2}}\,\frac{d_e}{w}$$

✓ fast reconnection in non-relativistic, magnetically dominated pair plasmas is possible in collisionless regimes even in the absence of dispersive waves!

Two-Fluid (electron + ion) Reconnection

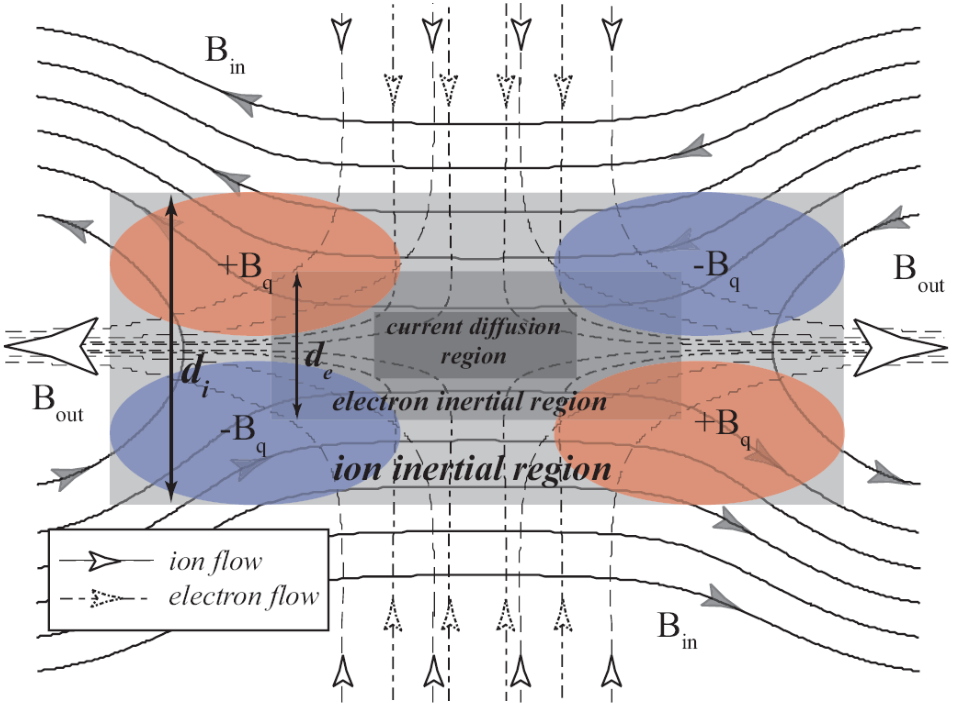

✓ presence of multiple scales in the physical system may result in decoupling of the in-plane flow and out-of-plane current diffusion scales within the reconnection region;

✓ no *a priory* known way to determine how many scales along the inflow and outflow directions, respectively, should be considered – difficult to design an appropriate Sweet-Parker-like model.

Two-Fluid (electron + ion) Reconnection

Uniform density, incompressible, two-fluid MHD:

$$
\begin{aligned}
\frac{d\mathbf{v_i}}{dt} + \epsilon \frac{d\mathbf{v_e}}{dt} &= \frac{1}{d_i}(\mathbf{v_i} - \mathbf{v_e}) \times \mathbf{B} - \nabla(p_i + p_e) + \nabla^2(\mu_i \mathbf{v_i} + \mu_e \mathbf{v_e}) \\
\epsilon d_i \frac{d\mathbf{v_e}}{dt} + \mathbf{E} &= -\mathbf{v_e} \times \mathbf{B} - \nabla p_e + \frac{\eta}{d_i}(\mathbf{v_i} - \mathbf{v_e}) + d_i \mu_e \nabla^2 \mathbf{v_e} \\
\nabla \times \mathbf{B} &= \frac{1}{d_i}(\mathbf{v_i} - \mathbf{v_e}) \\
\nabla \times \mathbf{E} &= -\frac{\partial \mathbf{B}}{\partial t},
\end{aligned}
$$

where:

$\epsilon \equiv \frac{m_e}{m_i}$ is the electron-to-ion mass ratio,
d_i is the ion inertial scale,
μ_i and μ_e are the ion and electron viscosity coefficients, and
η is the collisional resistivity coefficient.

Two-Fluid (electron + ion) Reconnection

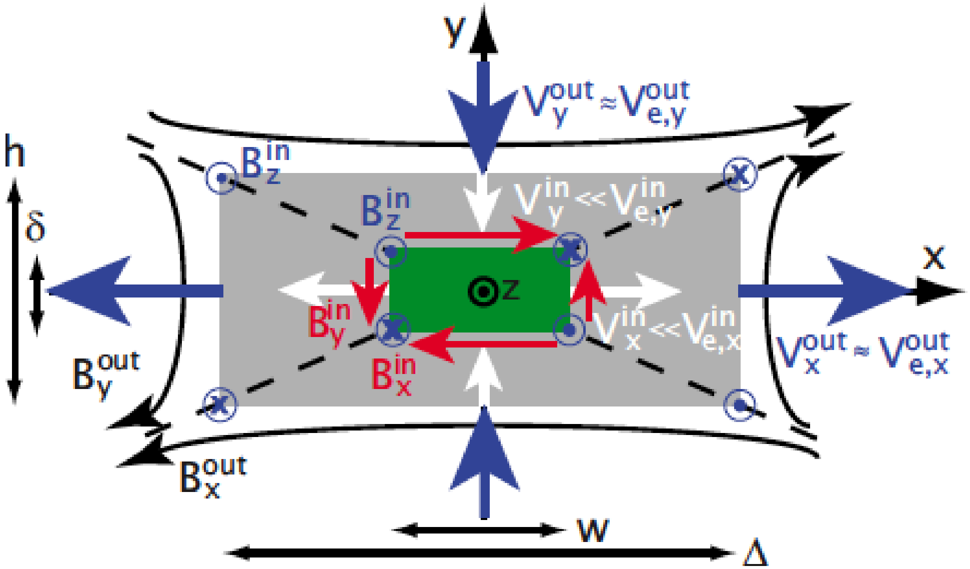

Sweet-Parker-like model
for incompressible Hall MHD
(2-fluid less electron inertia)
Simakov and Chacon (2008)

$$E_R = \frac{B_x^{in}(1-\xi^2)}{w\xi}\left[\eta + \Lambda\frac{\nu}{w^2}\left(1+\frac{1}{\xi^2}\right)\right]$$

where $\xi \equiv (\delta/w)$ and $\Lambda \approx 10-20$.

Later extended to include electron inertia by Malyshkin, PRL (2009)

Two-Fluid (electron + ion) Simulation

Magnetic Flux

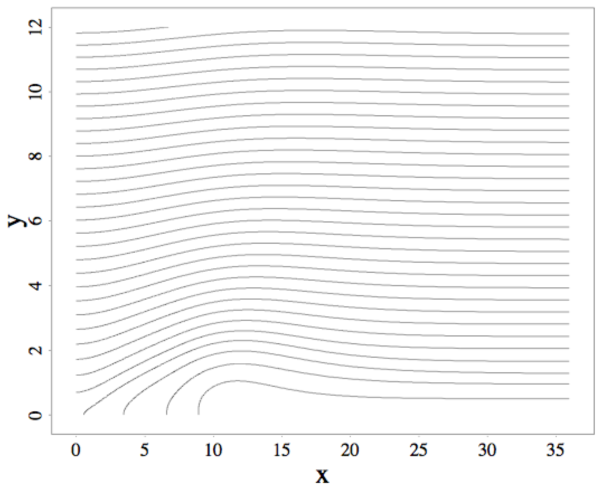

Reconnection Rate

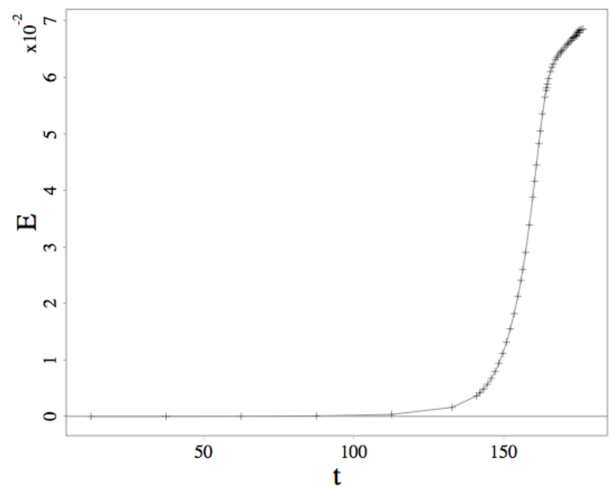

<u>Simulation parameters</u>:

$$d_i = 0.5$$
$$\epsilon = 5.446 * 10^{-4}$$
$$\eta = 10^{-4}$$
$$\mu_i = 10^{-4}$$
$$\mu_e = 10^{-6}$$

Current Density Profiles Across & Along the Reconnection Region

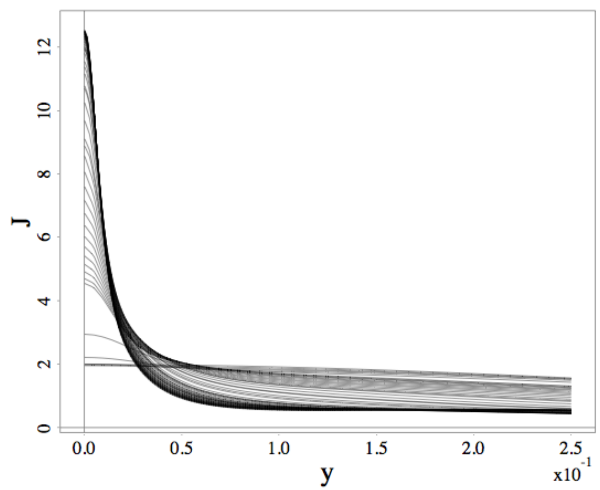

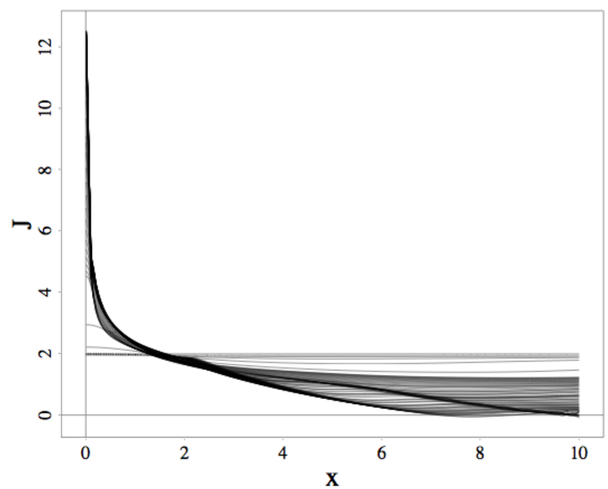

- ✓ The current sheet aspect ratio is again L/δ ~ 10, similar to Model-II of Anomalous Resistivity, but its dimensions are an order of magnitude smaller;
- ✓ Electron viscosity and inertia are the defining parameters for the two-fluid reconnection layer.

Two-Fluid (plasma + neutral) Reconnection

- Weakly ionized magnetized plasmas are subject to magnetic reconnection in the solar chromosphere, interstellar medium, etc. Presently being explored in the MRX experiment;

- Use the two-fluid approach, one fluid is plasma (i), the other is neutrals (n). Include electron impact ionization, radiative recombination, ion-neutral collisional friction and heat exchange. Assume single ionization and charge neutrality:

$$\text{Ion continuity: } \frac{\partial n_i}{\partial t} + \nabla.(n_i \mathbf{v}_i) = \Gamma_i^{ion} - \Gamma_n^{rec}$$

$$\text{Ion momentum: } \frac{\partial}{\partial t}(m_i n_i \mathbf{v}_i) + \nabla.(m_i n \mathbf{v}_i \mathbf{v}_i + pI + \pi) =$$

$$\mathbf{j} \wedge \mathbf{B} + R_i^{in} + \Gamma_i^{ion} m_i \mathbf{v}_n - \Gamma_n^{rec} m_i \mathbf{v}_i$$

$$\text{Ohm's law: } \mathbf{E} + (\mathbf{v}_i \wedge \mathbf{B}) = \eta \mathbf{j}$$

Two-Fluid (plasma + neutral) Simulation

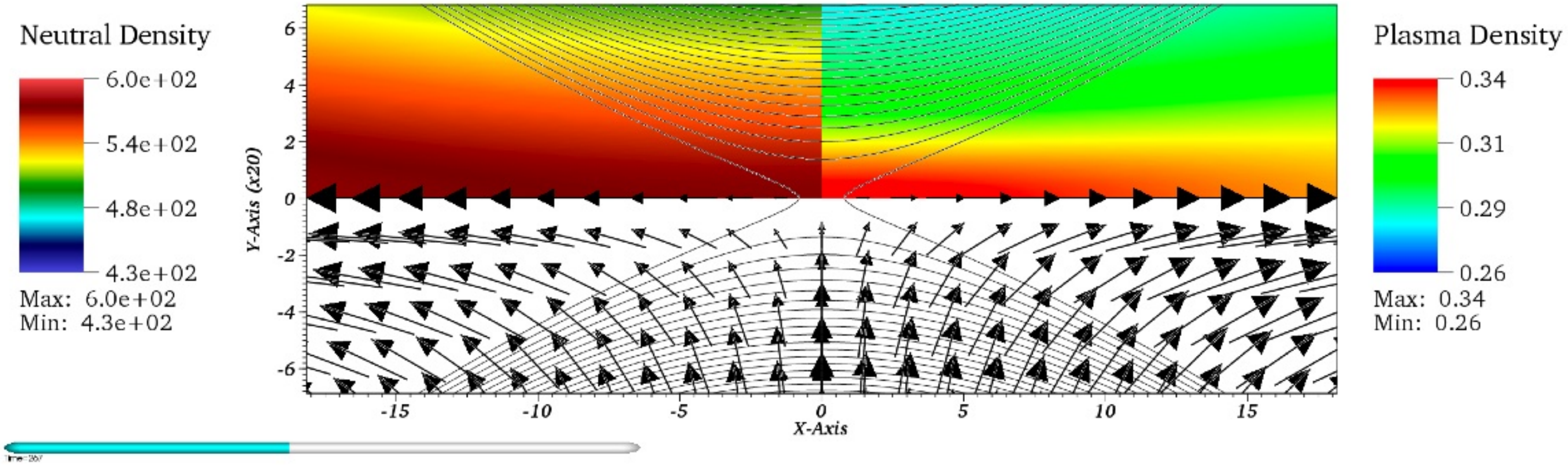

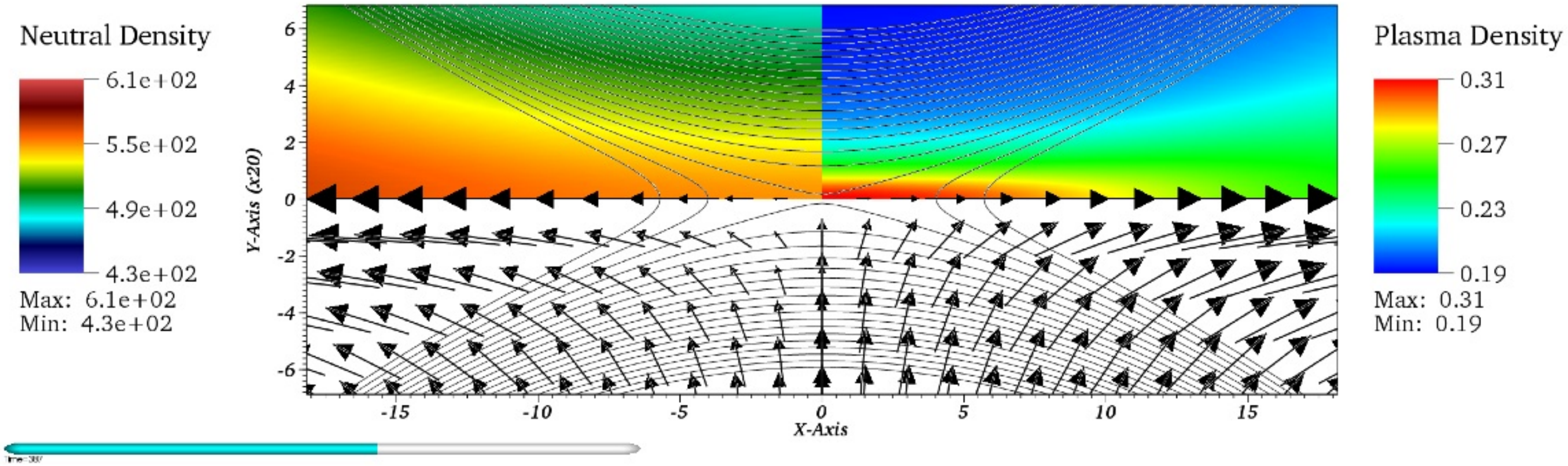

Two-Fluid (plasma + neutral) Simulation

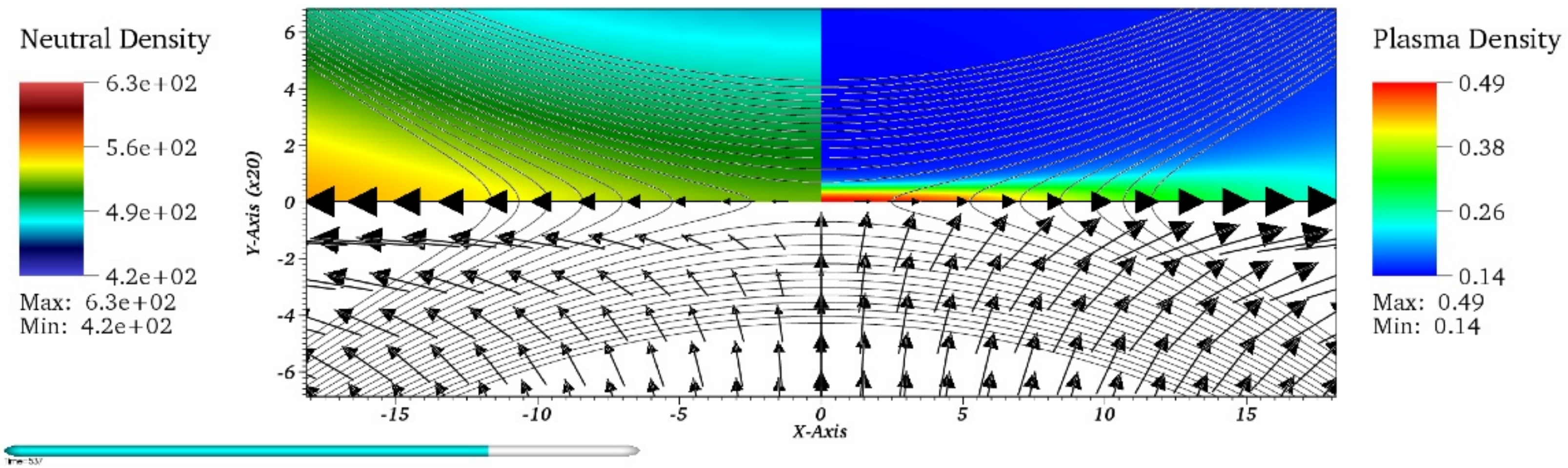

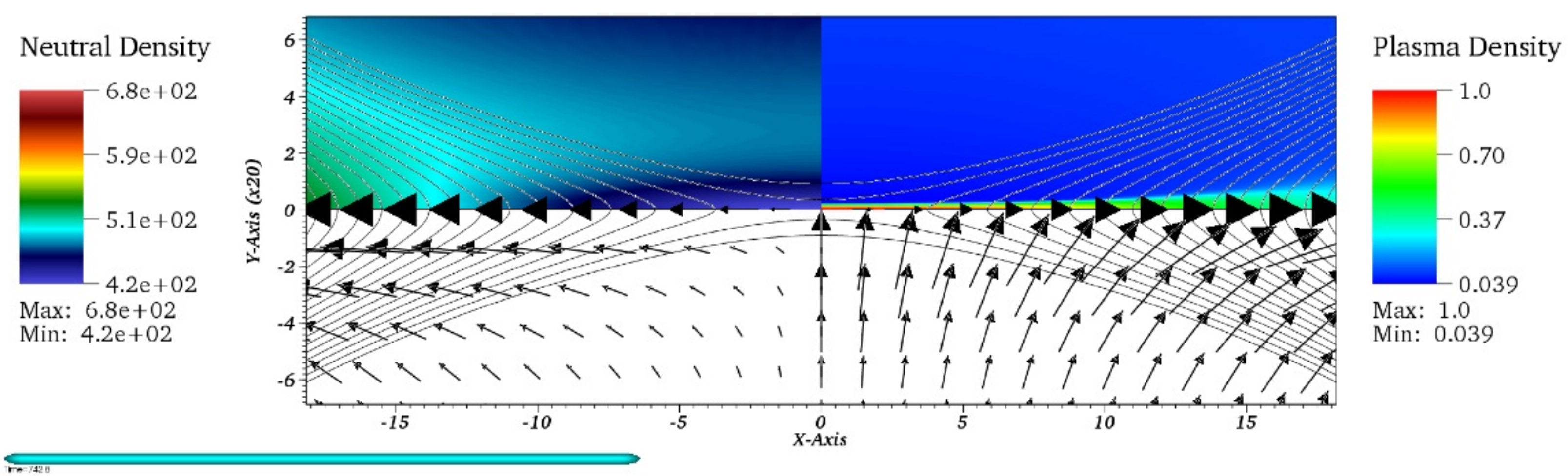

Two-Fluid (plasma + neutral) Simulation

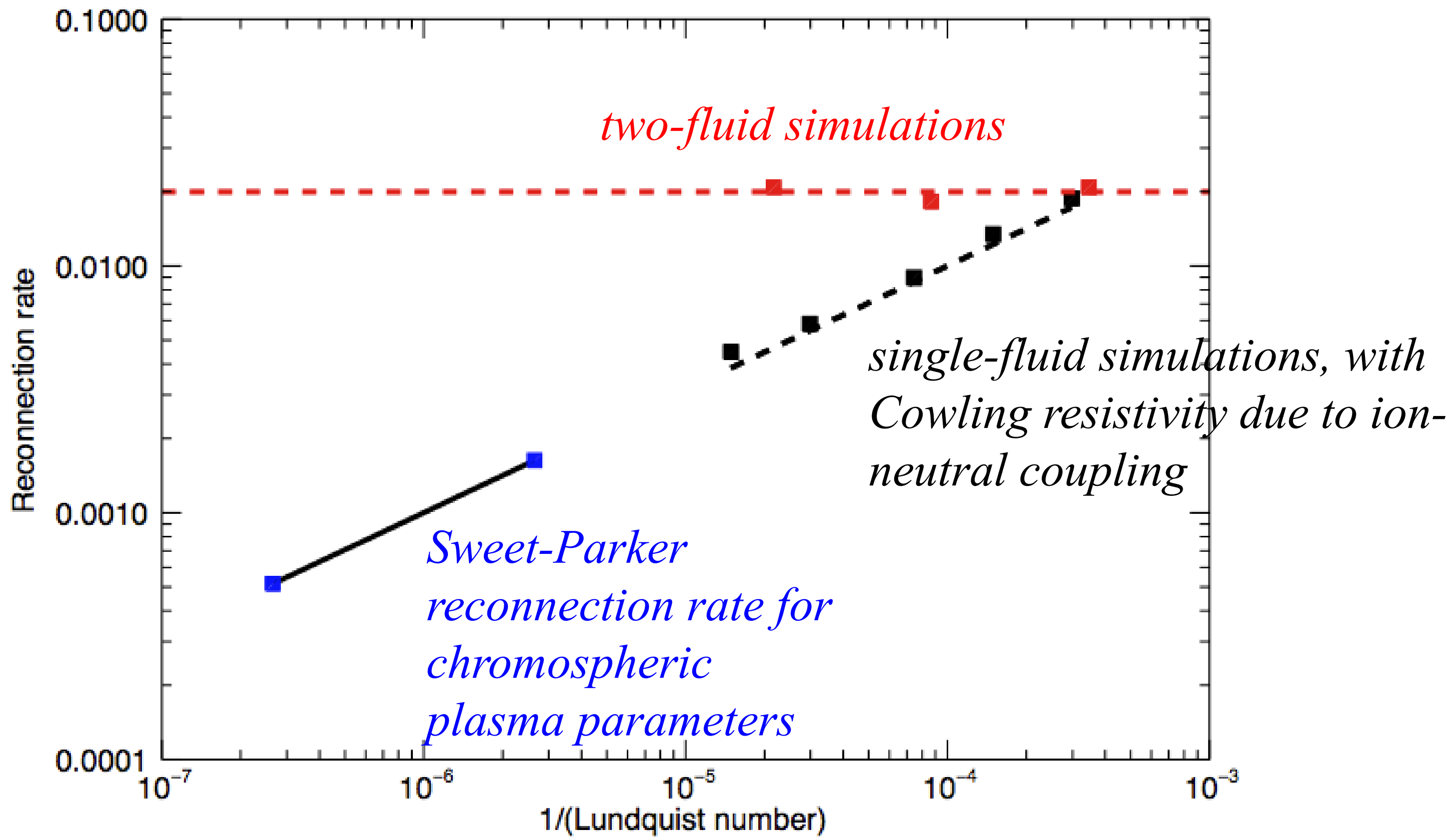

Plot courtesy of James Leake

✓ This system shows pronounced decoupling in the inflow, but no decoupling in the outflow. Yet, reconnection rate appears to be independent of resistivity; here it is due to build-up and resulting rapid recombination of plasma in the current layer, as has been previously conjectured by Heitsch & Zweibel, ApJ (2003).

3D System Simulation

Two co-axial spheromaks of the same helicity situated next to each other in a cylindrical flux conserver, such that their poloidal B-fields are co-directed at the midplane and their interior toroidal B-fields are oppositely directed.

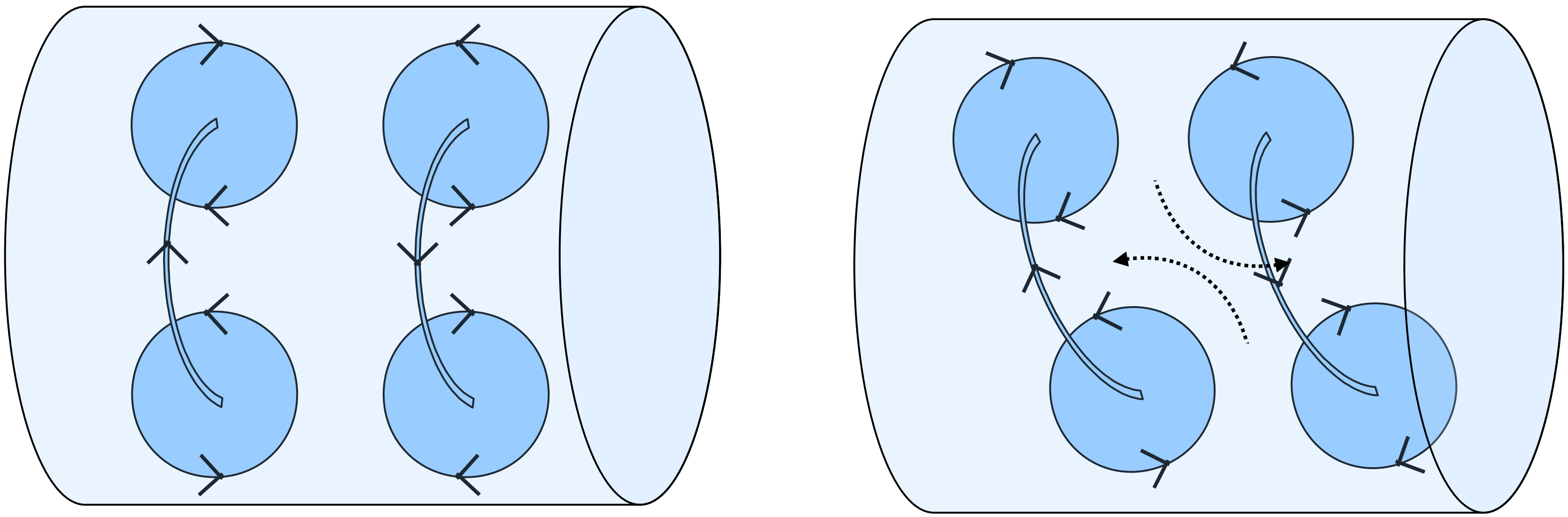

- There is a single interior B-field null point at the center between the two spheromaks;
- Co-directed tilting is initially accompanied by magnetic reconnection of poloidal B-fields between the top portion of one and the bottom of the other spheromak at the null point;
- It is all 3D reconnection and relaxation from there on out...

Partial Differential Equations

3D Compressible (Hall) MHD

$$\frac{\partial \tilde{\rho}}{\partial \tilde{t}} + \tilde{\nabla} \cdot [\tilde{\rho} \tilde{\mathbf{v}}_i] = 0 \qquad (1)$$

$$\frac{\partial (\tilde{\rho} \tilde{\mathbf{v}}_i)}{\partial \tilde{t}} + \tilde{\nabla} \cdot \left[\tilde{\rho} \tilde{\mathbf{v}}_i \tilde{\mathbf{v}}_i + \tilde{p} \tilde{\mathbf{I}} - \mu_i \tilde{\nabla} \tilde{\mathbf{v}}_i - \mu_e \tilde{\nabla} \tilde{\mathbf{v}}_e \right] = \tilde{\mathbf{J}} \times \tilde{\mathbf{B}} \qquad (2)$$

$$\tilde{\mathbf{E}} = -\frac{\partial \tilde{\mathbf{A}}}{\partial \tilde{t}} = -\tilde{\mathbf{v}}_e \times \tilde{\mathbf{B}} - \frac{d_i}{\tilde{\rho}} \tilde{\nabla} \tilde{p}_e + \mathbf{D}_J \qquad (3)$$

$$\frac{3}{2} \frac{\partial \tilde{p}}{\partial \tilde{t}} + \tilde{\nabla} \cdot \left[\frac{5}{2} (\tilde{p}_i \tilde{\mathbf{v}}_i + \tilde{p}_e \tilde{\mathbf{v}}_e) - \kappa \tilde{\nabla} \tilde{T} \right] \qquad (4)$$

$$= \tilde{\mathbf{v}}_i \cdot \tilde{\nabla} \tilde{p}_i + \tilde{\mathbf{v}}_e \cdot \tilde{\nabla} \tilde{p}_e + \mu_i ||\tilde{\nabla} \tilde{\mathbf{v}}_i||^2 + Q_J \qquad (5)$$

where

$$\tilde{\mathbf{B}} = \tilde{\nabla} \times \tilde{\mathbf{A}}, \qquad \tilde{\mathbf{J}} = \tilde{\nabla} \times \tilde{\mathbf{B}} = \tilde{\nabla}(\tilde{\nabla} \cdot \tilde{\mathbf{A}}) - \tilde{\nabla}^2 \tilde{\mathbf{A}}$$

$$\tilde{\mathbf{v}}_e = \frac{\tilde{\rho} \tilde{\mathbf{v}}_i - d_i \tilde{\mathbf{J}}}{\tilde{\rho}},$$

$$\tilde{p} = \tilde{\rho} \tilde{T} = \tilde{p}_i + \tilde{p}_e, \qquad \frac{\tilde{p}_e}{\tilde{p}_i} = \text{const},$$

$$\mathbf{D}_J = \begin{cases} (d_i \mu_e / \tilde{\rho}) \tilde{\nabla}^2 \tilde{\mathbf{v}}_e, & d_i > 0 \\ -\nu \tilde{\nabla}^2 \tilde{\mathbf{J}}, & d_i = 0 \end{cases},$$

$$Q_J = \begin{cases} \mu_e ||\tilde{\nabla} \tilde{\mathbf{v}}_e||^2, & d_i > 0 \\ \nu ||\tilde{\nabla} \tilde{\mathbf{J}}||^2, & d_i = 0 \end{cases},$$

Global Merging Evolution

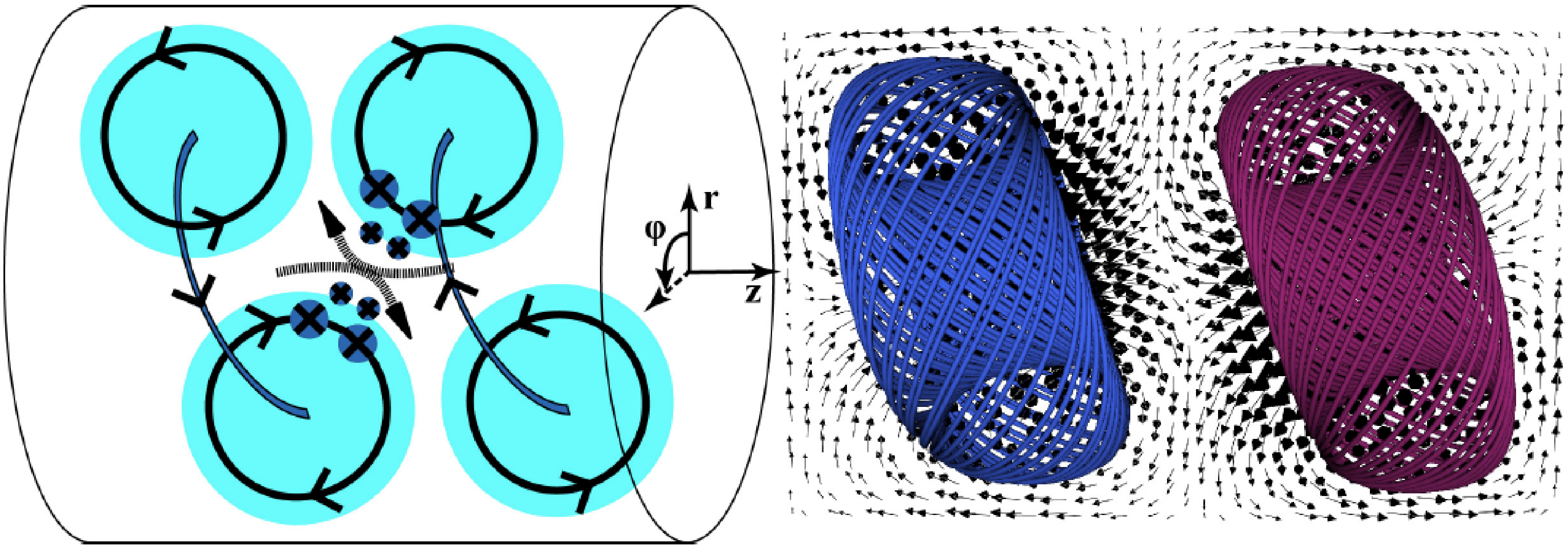

Fig. 1. A cartoon (left panel) and HiFi simulation (right panel) of two tilting spheromaks undergoing magnetic reconnection at the central magnetic null. The cartoon indicates the reconnecting in-plane **B**-field components and the co-directed out-of-plane **B**-field being convected into the RR. The simulation panel shows streamlines of two separate magnetic field-lines, and arrows show the magnetic field direction and strength at the mid-plane. Note that the two spheromaks have oppositely directed toroidal magnetic fields.

Lukin & Linton, Nonlinear Proc. Geophys. (2011).

Global Merging Evolution

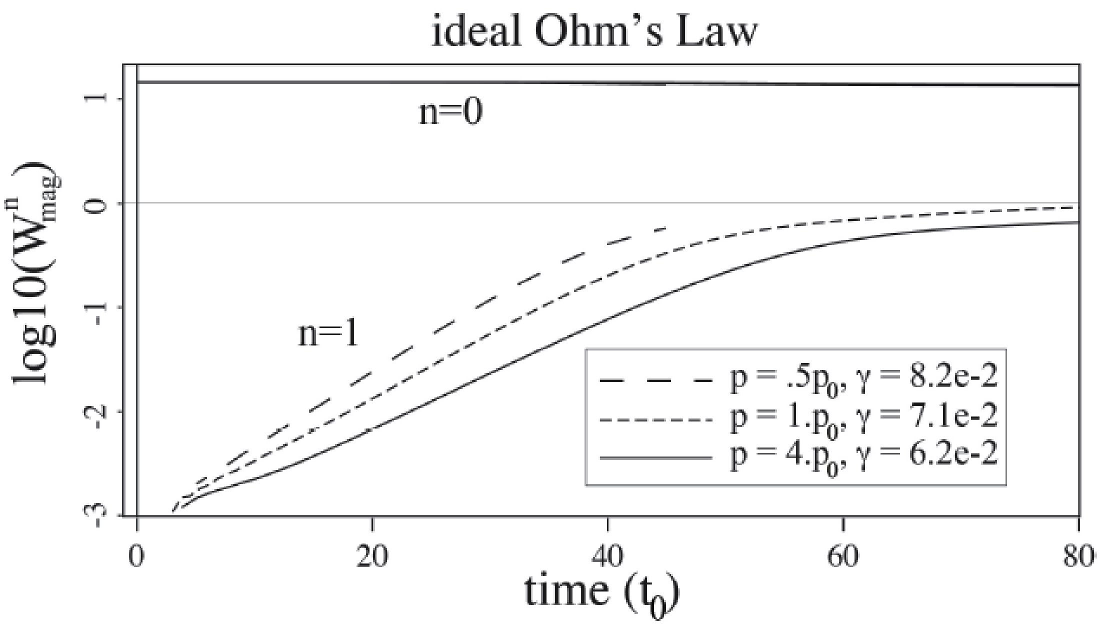

- Without magnetic dissipation, the system relaxes to a slightly more favorable energy state by allowing the spheromaks to tilt through onset and saturation of the n=1 tilt mode. However most of the energy remains in the axisymmetric state.

Fig. 2. Time-traces of normalized magnetic energy W^n_{mag} in $n = 0$ and $n = 1$ modes for three simulations with different values of initial pressure $p|_{t=0} = 0.5p_0, 1p_0, 4p_0$ all conducted with no magnetic dissipation ($\mathbf{D}_J = \mathbf{0}$) in the single-fluid regime ($d_i = 0$). The corresponding normalized linear growth rate γ of the tilt mode converting W^0_{mag} energy into W^1_{mag} energy is shown in the legend for each of the three cases.

Global Merging Evolution

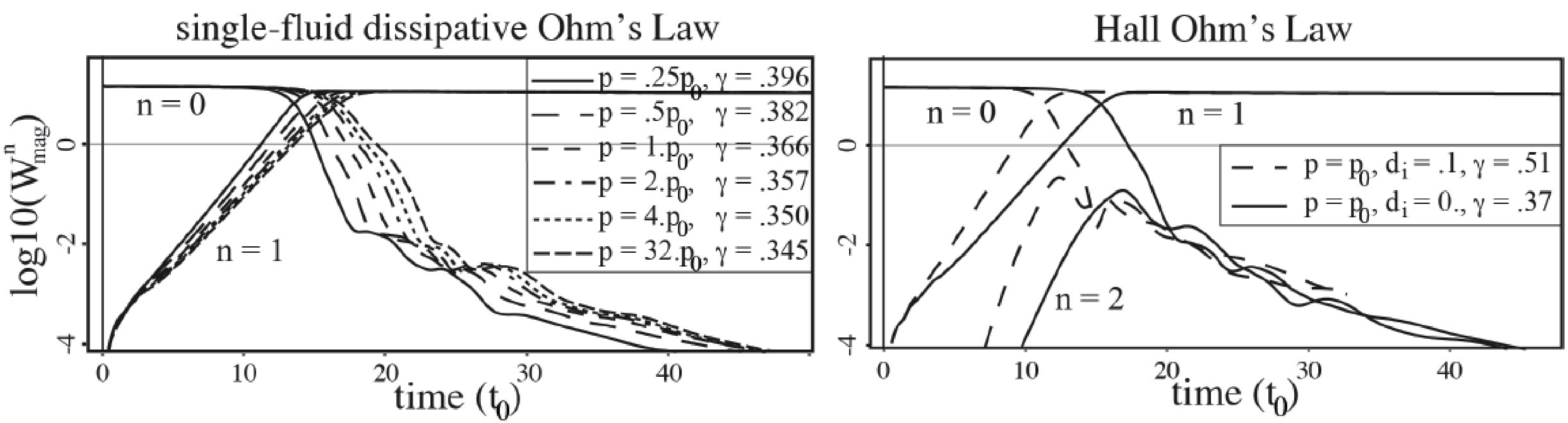

Fig. 3. Comparison of time-traces of ϕ-mode magnetic energy W^n_{mag} for several simulations (left) with different values of initial pressure $p|_{t=0}$ conducted in the single-fluid mode with finite magnetic dissipation ($d_i = 0$, $\nu = 5 \times 10^{-6}$), and (right) both with and without the Hall effect for the same value of initial plasma pressure and finite magnetic dissipation ($d_i^2 \mu_e = \nu = 5 \times 10^{-6}$). The corresponding normalized linear growth rate γ of the $n = 1$ mode is shown in the legend for each of the simulations.

Global Merging Evolution

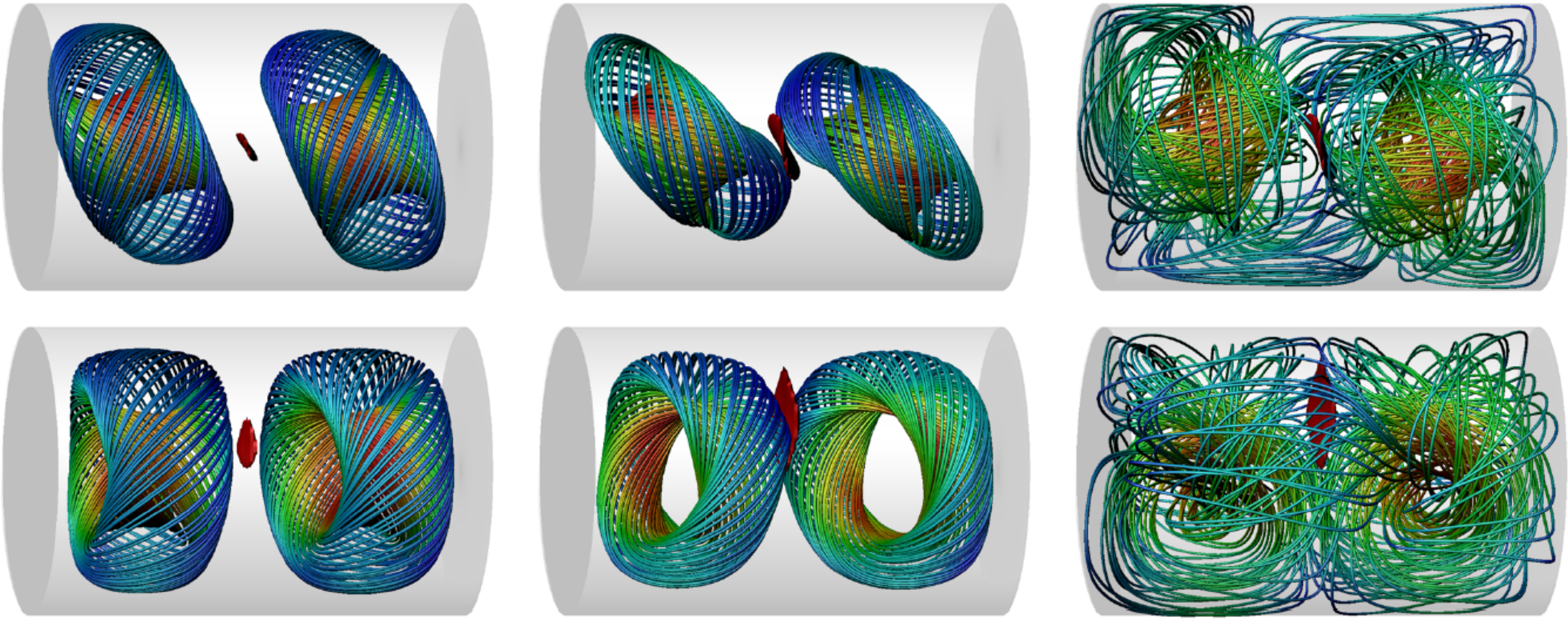

Magnetic Field Streamlines & Surface of High Current Density
(top and bottom rows are rotated by 90 degrees with respect to each other)
[Gray *et al.*, PoP (2010)]

Reconnection Region

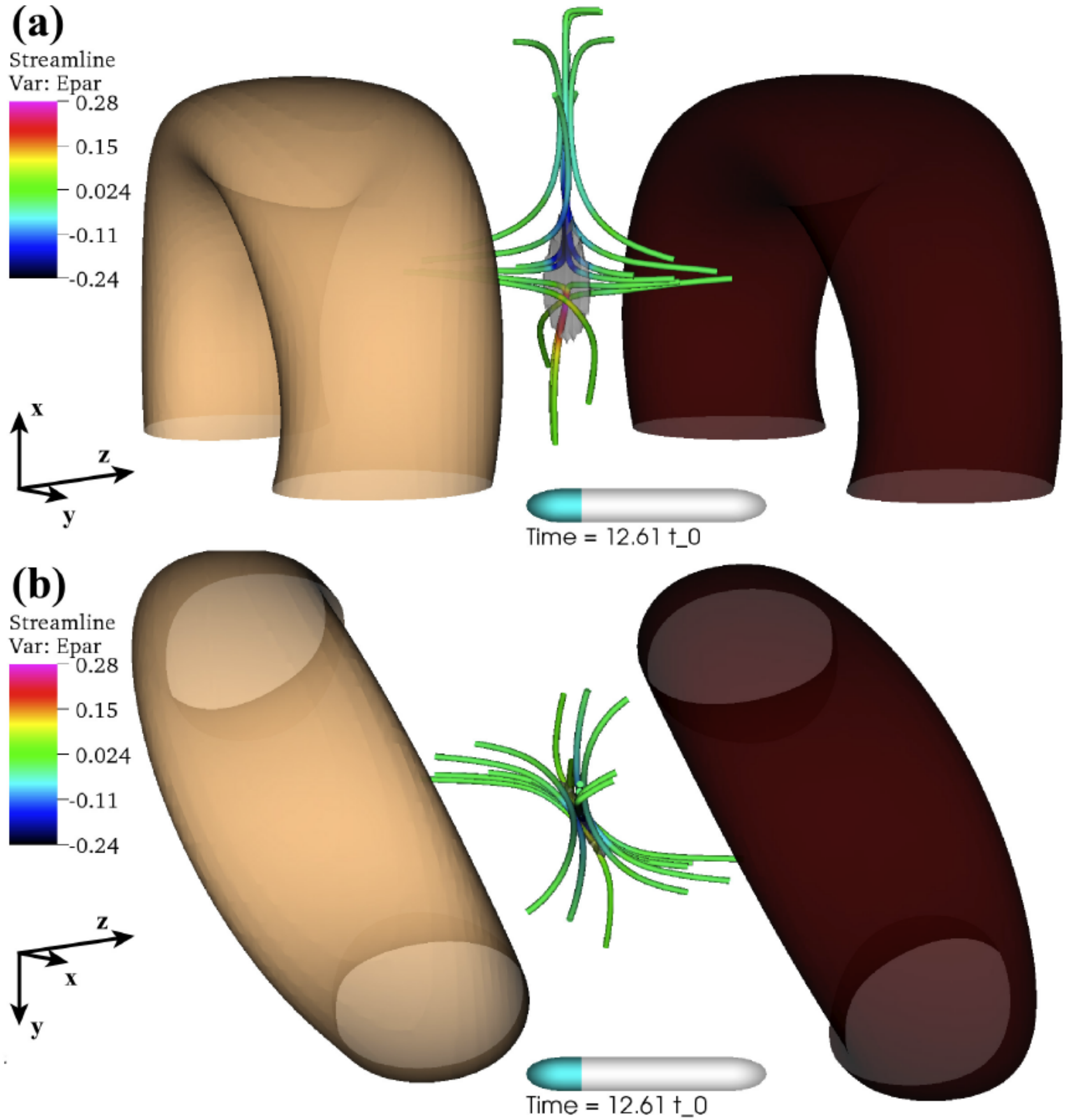

- Light and dark brown surfaces are those of constant A_φ, approximating magnetic flux surfaces for visualization purposes;
- Streamlines around the null are select magnetic field lines with the color showing parallel **E**-field Epar =**E.B**/|**B**| at each location along the field lines;
- Grey surface in the center of the null is that of enhanced current density associated with ongoing magnetic reconnection.

Reconnection Region: Null Motion

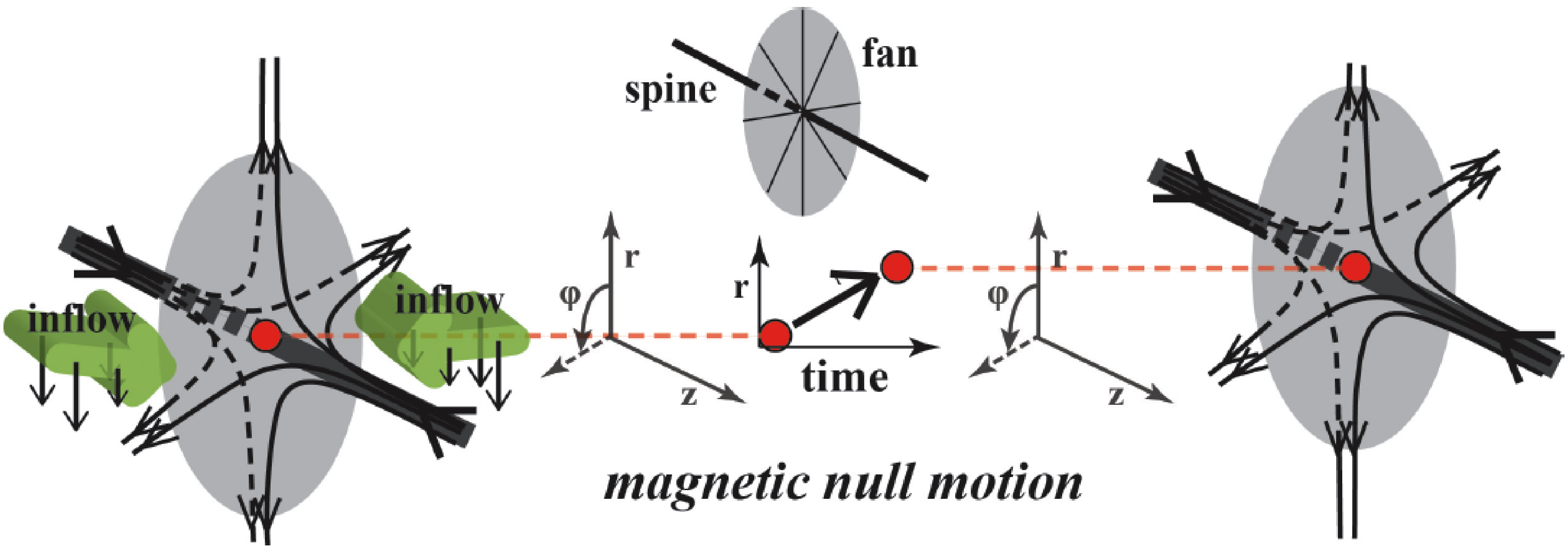

Fig. 6. Schematic of the spine-fan magnetic null centered between the two spheromaks. As the symmetry of the null is broken and magnetic reconnection commences, in-plane plasma flows carry into the null the component of magnetic field perpendicular to the reconnection plane. These field components, originally the toroidal fields of the spheromaks, are co-aligned and combine with corresponding components of the fan magnetic field around the null. As a result, the magnetic null moves along a radial cord in the plane of the fan and normal to the reconnection plane.

Reconnection Region: Structure

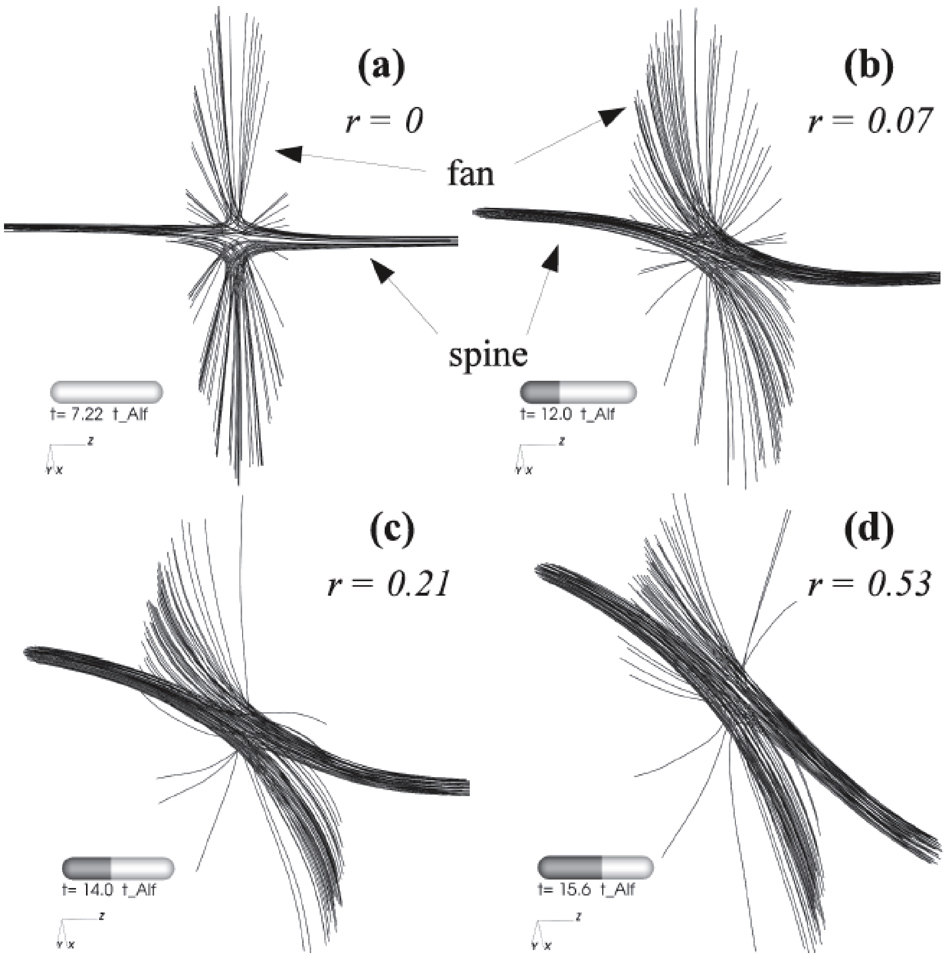

Spine-fan magnetic field structure surrounding the magnetic null point

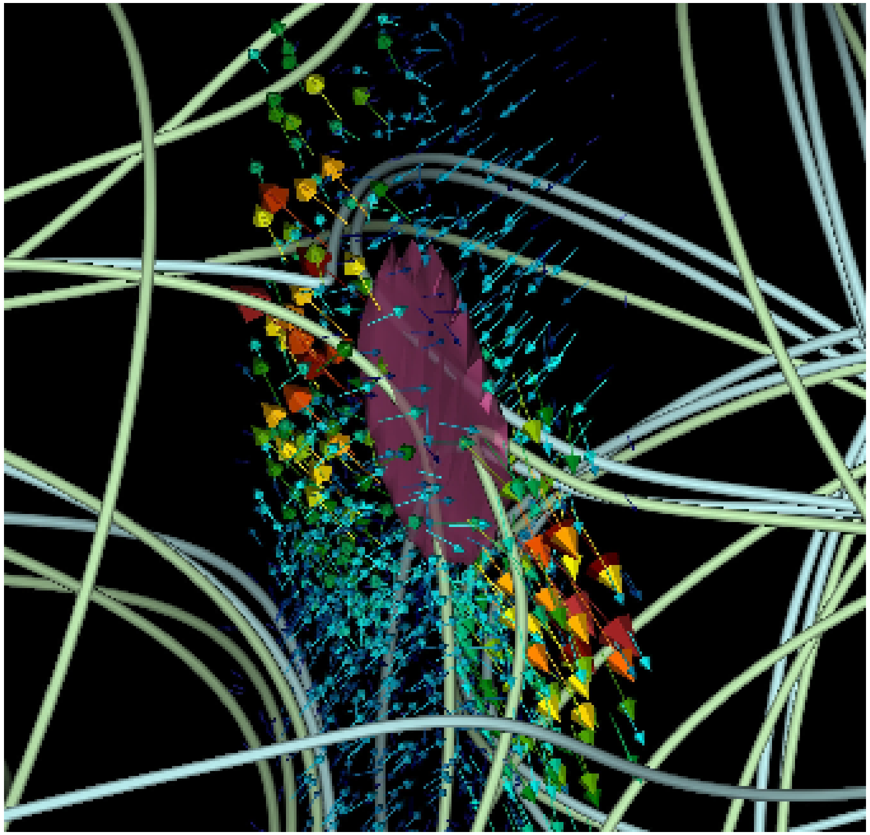

At each time, in a suitably chosen plane, reconnection geometry looks quasi two-dimensional

Reconnection Region: Reconnection Rate

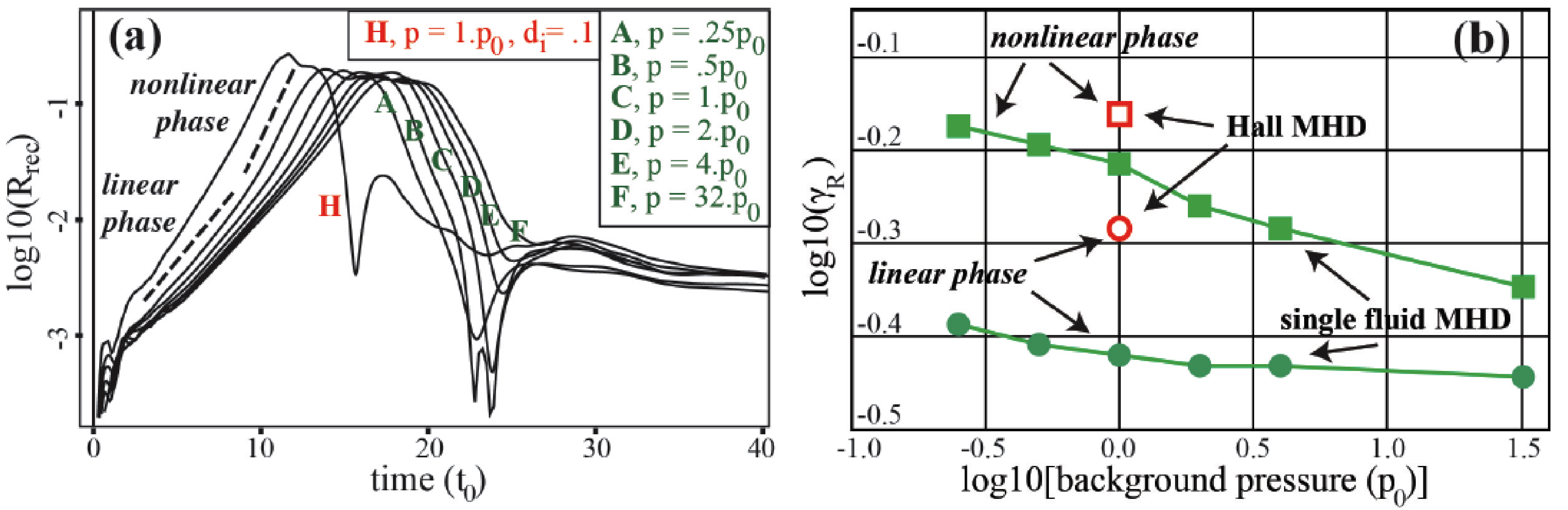

Fig. 8. (**a**) Time traces of normalized reconnection rate R_{rec} for the six single-fluid MHD simulations with varying plasma β (labeled **A**–**F**) and the Hall MHD simulation (labeled **H**) described in Fig. 3. (**b**) The effective growth rate γ_R of R_{rec} versus the background pressure in the early linear and late nonlinear phases of reconnection.

Reconnection Region & Null Motion Correlation

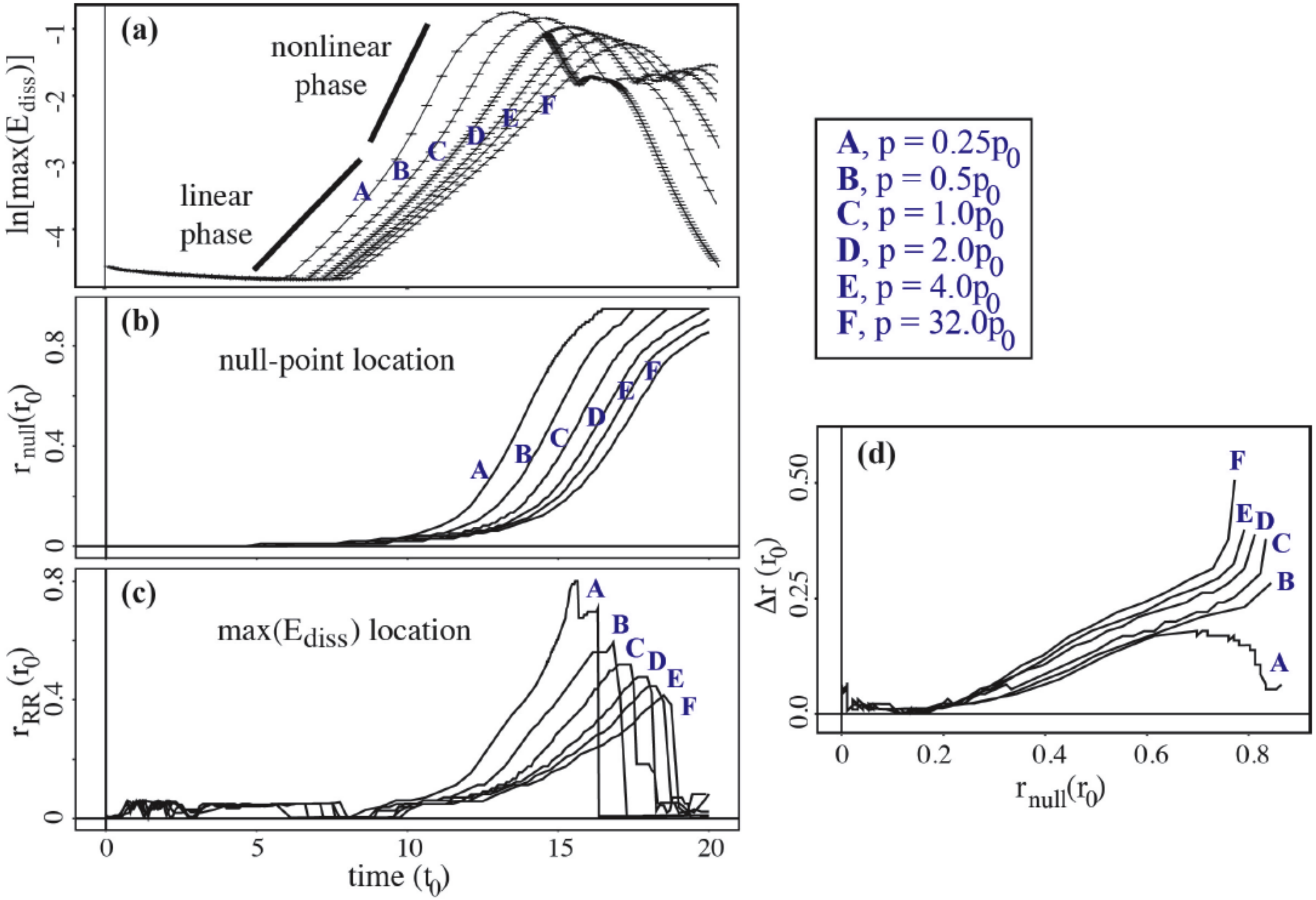

Fig. 9. Time traces of (**a**) the maximum magnitude of normalized dissipation electric field $\max(E_{\text{diss}})$; (**b**) the radial position of the magnetic null-point r_{null} and (**c**) the radial position of the location of maximum dissipation **E**-field r_{RR} for the six single-fluid simulations with varying plasma β. Panel (**d**) shows the radial distance $\Delta r \equiv (r_{\text{null}} - r_{\text{RR}})$ versus the null-point's radial position r_{null}.

Fast 3D Reconnection?

Assume a 3-D localized reconnection region (RR) of some width determined by the non-ideal magnetic dissipation processes, length L_{RR} along the reconnection outflow direction, and some height H_{RR} along the direction of reconnection current. Also, assume that the magnetic field configuration of the RR is moving at some velocity $\mathbf{v}_{\mathbf{RR}}$ along the direction of the reconnection current. Then, in steady state, in the moving frame of reference of the RR:

$$\frac{dL_{\mathrm{RR}}}{dt} = \frac{\partial L_{\mathrm{RR}}}{\partial \tilde{t}} + \mathbf{v}_{\mathrm{RR}} \cdot \nabla L_{\mathrm{RR}} = 0$$

$$\Rightarrow L_{\mathrm{RR}} \approx \frac{v_{el}}{v_{\mathrm{RR}}} \frac{H_{\mathrm{RR}}}{2},$$

where $v_{el} \equiv (\partial L_{\mathrm{RR}} / \partial t)$ is the rate of nonlinear elongation of a 2-D reconnection current layer in the stationary frame of reference.

Since v_{el} and v_{RR} can both be large fractions of the Alfven speed, i.e. $(v_{el}/v_{RR}) \sim 1$, it follows that $L_{RR}/H_{RR} \sim 1$.

This could resolve the bottleneck of the 2D Sweet-Parker reconnection...